frontiers in Space Technologies

TYPE Original Research
PUBLISHED 18 March 2026
DOI 10.3389/frspt.2026.1791484

OPEN ACCESS

EDITED BY
Timothy Grant Hammond,
Duke University, United States

REVIEWED BY
Romain Briandet,
Institut National de recherche pour l'agriculture, l'alimentation et l'environnement (INRAE), France
Daniele Marra,
University of Naples Federico II, Italy

*CORRESPONDENCE
Jamie S. Foster,
jfoster@ufl.edu

†PRESENT ADDRESS
Eric J. Koch,
Observatoire Océanologique de Banyuls-sur-mer, Banyuls-sur-mer, France

RECEIVED 19 January 2026
REVISED 09 February 2026
ACCEPTED 10 February 2026
PUBLISHED 18 March 2026

CITATION
Koch EJ, Conesa A, Garrett TJ, Ormsby R, Bohl R, Reed DW and Foster JS (2026) Beneficial microbes mitigate molecular stress responses and accelerate developmental pathways in host animals during spaceflight.
Front. Space Technol. 7:1791484.
doi: 10.3389/frspt.2026.1791484

Beneficial microbes mitigate molecular stress responses and accelerate developmental pathways in host animals during spaceflight

Eric J. Koch [1†], Ana Conesa [2], Timothy J. Garrett [3], Rachel Ormsby[4], Ryan Bohl[4], David W. Reed[4] and Jamie S. Foster [1*]

[1]Department of Microbiology and Cell Science, Space Life Science Lab, University of Florida, Merritt Island, FL, United States, [2]Spanish National Research Council, Institute for Integrative Systems Biology, Valencia, Spain, [3]Department of Pathology, Immunology and Laboratory Medicine, College of Medicine, University of Florida, Gainesville, FL, United States, [4]Redwire Space Technologies, Inc., Greenville, IN, United States

As humans continue the manned exploration of space, it is critical to understand the impact of this harsh environment on the beneficial microbes that interact with their bodies. Here, we explore whether the onset of symbiotic associations between microbes and animals are impacted during spaceflight. We used the association between the bobtail squid *Euprymna scolopes* and its beneficial bacterium *Vibrio fischeri* as an animal model system to examine how spaceflight affects symbiotic interactions at the transcriptomic, metabolomic, and lipidomic levels over time. Our results suggest that in the spaceflight environment, symbiotic microbes can mitigate molecular stress responses of the host animal and accelerate normal developmental pathways, such as neurogenesis and tissue morphogenesis. Overall, this work provides evidence that beneficial microbes can effectively colonize nascent host epithelial tissues in microgravity and play a critical role in shaping the host tissue environment to promote stability of symbiosis during spaceflight.

KEYWORDS
animal development, host-microbe interactions, microgravity, spaceflight, symbiosis

1 Introduction

Spaceflight exerts numerous environmental and physiological challenges on life. Whether it be the reduction of gravity, increased exposure to radiation, or the mental health challenges of being in a confining and isolating environment (Durante and Cucinotta, 2008; Blaber et al., 2010; Afshinnekoo et al., 2020), working and living in space presents unique challenges to not only plant and animal hosts but also their associated microbiomes (Foster et al., 2014; Tesei et al., 2022). Eukaryotes live in a microbial world, and space travel is no exception. Microbes are transported and exchanged with the crew, food supplies, experimental cargo, flight hardware, and the spacecraft itself; however, the processes by which interdomain communication is happening in the spaceflight ecosystem are not fully understood and represent an important area of research for on-going human spaceflight activities.

Recently, there have been numerous studies on how the dynamics and diversity of the microbiome change within and amongst astronauts as well as the exchange between the crew

and the built environment of the International Space Station (ISS) (Garrett-Bakelman et al., 2019; Jiang et al., 2019; Mora et al., 2019; Voorhies et al., 2019; Avila-Herrera et al., 2020; Liu et al., 2020; Urbaniak et al., 2020; Chen et al., 2021; Morrison et al., 2021; Bedree et al., 2023; Tierney et al., 2024). The results of these studies have been varied and appear to be highly dependent on the location within the body, with increased taxonomic diversity even after short exposures to space in the gut and saliva microbiomes, whereas other areas maintain homeostasis over time, such as the skin microbiome (Tesei et al., 2022). The changes in microbiome diversity and associated metabolism can be heavily influenced by additional modifiers, such as diet, age, medications, and flight durations (Garrett-Bakelman et al., 2019; Jiang et al., 2019; Voorhies et al., 2019). Although efforts are underway to regularly track and monitor the microbiomes of crew and spacecraft to improve the overall understanding of what is a healthy microbiome during spaceflight (Lee et al., 2021; Urbaniak et al., 2022), there are numerous unresolved questions including what drives the variation of the host microbiome in space and how resilient the microbiome is to the many hazards of spaceflight. Additionally, due to the overall complexity of the microbiome, fundamental questions persist regarding whether spaceflight alters the normal communication between host animal tissues and their associated microbes and how beneficial microbes facilitate and mediate the normal development of animals in environmentally stressful conditions.

One approach to address these fundamental questions of how microbes, particularly beneficial microbes, impact the normal health and development of animals during spaceflight is to use simplified model systems. As in Earth-based research, it is necessary to use multiple model systems in space biology research to generate a robust understanding of the impact that spaceflight has on animal-microbe communication and physiology. No single model system can address all questions regarding the impact of spaceflight on animal and human health (Ruby, 2008; McFall-Ngai and Bosch, 2021). Although there has been significant progress regarding the use of tissue and organoid chips for spaceflight experiments (Low and Giulianotti, 2019; Puschhof et al., 2021; Parafati et al., 2023), there are still significant limitations for examining complex organismal-level functions throughout the body as well as temporal and spatial variations between microbes and their hosts (Ingber, 2022), therefore using experimentally tractable animal-bacterial models that have short time frames of initiation and development are pivotal for space life sciences research.

In this study, we examined how microbes colonize nascent animal epithelial tissues under the physiological stress of spaceflight using the binary symbiosis between the Hawaiian bobtail squid *Euprymna scolopes* and its bioluminescent bacterial partner *V. fischeri*. The squid-vibrio symbiosis has served as a valuable model to help untangle the dynamic interplay between environmentally acquired bacteria, the host epithelial barrier, and the innate immune system for more than 30 years (McFall-Ngai and Ruby, 1991; Koch and McFall-Ngai, 2018; Essock-Burns et al., 2020; Koch et al., 2020a; Koch et al., 2020b; McFall-Ngai and Ruby, 2021; Essock-Burns et al., 2023). The squid harbors a specialized organ that houses the symbiosis and is embryologically derived from the squid hindgut (Montgomery and McFall-Ngai, 1993). The light organ exhibits both ciliated and microvillous epithelia, which are the two most common types of polarized mucosal epithelial within the animal kingdom that interface with bacterial symbionts (Nyholm et al., 2002; Nyholm and McFall-Ngai, 2021). Upon colonization, the light organ exhibits a mucosal innate immune response that shares extensive similarity to mammalian systems (Duscher et al., 2024). Additionally, previous research has shown that under simulated microgravity conditions wild-type strains of *Vibrio fischeri* do not exhibit noticeable changes to their growth rate compared to gravity-based controls (Vroom et al., 2021; Bongrand and Foster, 2023). Together, these features coupled with the small size of the hatchling squid (~3 mm, Figure 1a), short embryogenesis (~21 days), and rapid colonization and developmental timelines make this system ideal for spaceflight experimentation (Casaburi et al., 2017).

Within minutes of the squid hatching, microbes are recruited from the environment to the light organ surface (Figure 1b). Ciliated epithelial cells on the exterior of the light organ aggregate the bacteria into the vicinity of pores on the light organ surface that connect to six independent crypt spaces lined with mucosal epithelial cells (Figure 1c) (Nyholm et al., 2000; Nyholm and McFall-Ngai, 2004; Nawroth et al., 2017). Evidence suggests that regardless of inoculum size, typically only 1 *V. fischeri* cell is required to enter the pore and migrate to each of the six individual crypt spaces to initiate colonization (Wollenberg and Ruby, 2009; Bongrand et al., 2016). Once symbiosis-competent *V. fischeri* enter the crypt spaces they begin to replicate clonally and interact with the host epithelium (Bongrand and Ruby, 2019; Moriano-Gutierrez et al., 2020). During these interactions, the bacteria release diffusible molecules into the crypt spaces that can influence and modulate the host responses as well as foster communication between *V. fischeri* symbionts in the other crypt spaces (Septer and Stabb, 2012), thereby rapidly inducing host light organ morphogenesis (Montgomery and McFall-Ngai, 1994; Doino and McFall-Ngai, 1995; Foster and McFall-Ngai, 1998; Foster et al., 2000; Koch et al., 2014; Moriano-Gutierrez et al., 2019).

To explore how spaceflight impacts the onset of beneficial animal-microbe interactions, newly hatched squid were sent to the ISS aboard the SpaceX Commercial Resupply Services-22 mission (SpX-22) where, once in the microgravity environment, they were inoculated with mutualistic *V. fischeri*. The transcriptomes, metabolomes, and lipidomes of the juvenile squid, in the presence and absence of the beneficial microbes, were sampled over time to provide a broad overview of how spaceflight impacted the initiation of the symbiosis as well as the onset of bacteria-induced developmental pathways. The results of this study provide new insights into how the space environment alters the normal timeline of bacteria-induced developmental processes in host tissues and how microbes can potentially mitigate stress responses and promote the stability of symbiotic interactions following environmental perturbations, such as spaceflight.

2 Methods

2.1 Ethics statement

All experimental procedures using live cephalopods were approved by the University of Florida (201910899), NASA Flight (SQD01), and the Kennedy Space Center (FLT-20-129) Institutional

10.3389/frspt.2026.1791484

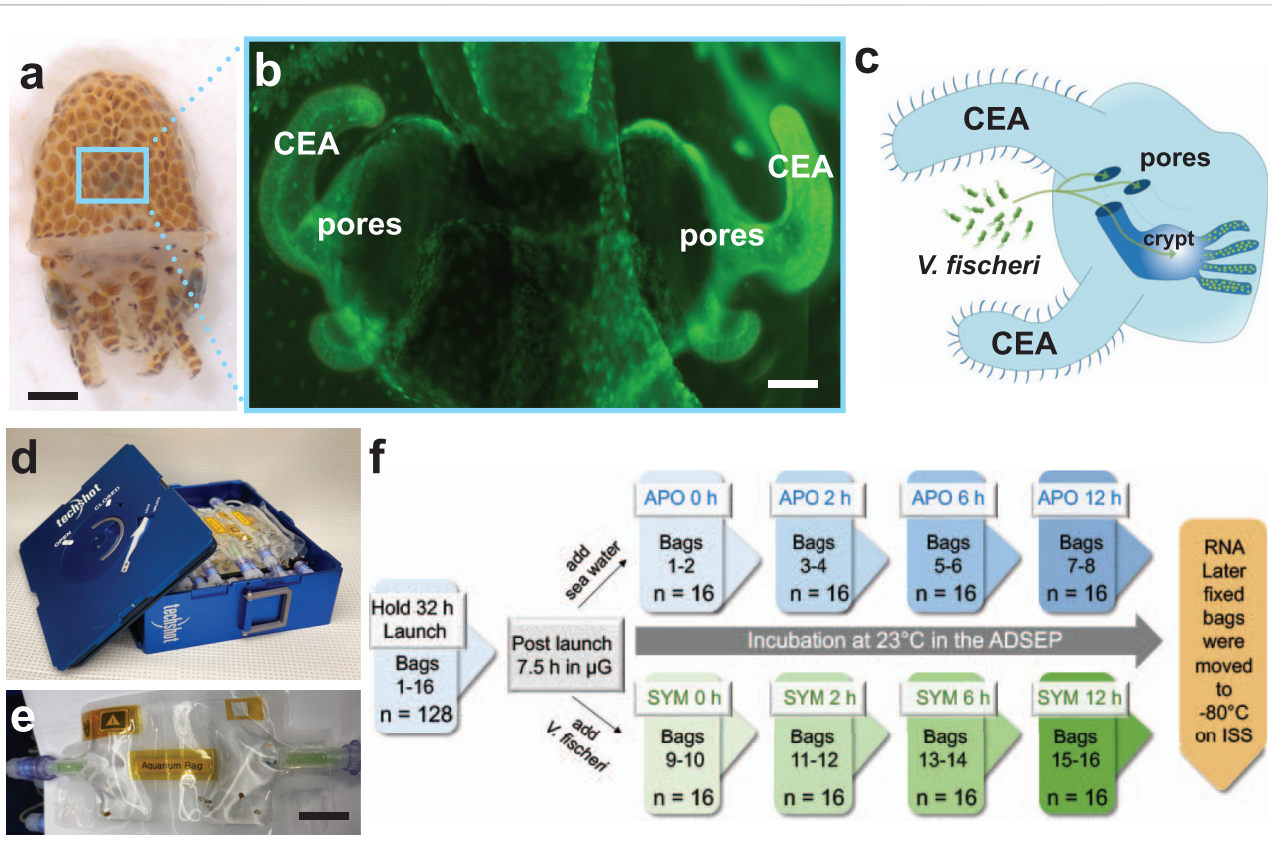

FIGURE 1
Overview of the squid-vibrio system and UMAMI experimental design. **(a)** Representative juvenile squid imaged after the completion of the UMAMI experiment. Blue box represents the location of the host light organ. Bar = 0.5 cm. **(b)** Representative epifluorescence image of light organ at the time of hatching depicting the pronounced ciliated epithelium appendage (CEA) structures on either side of the light organs that are used to recruit bacteria into the vicinity of pores on the surface of the light organ. Bar = 50 µm. **(c)** Cartoon of one-half of the light organ depicting the path symbiosis competent *Vibrio fischeri* travel to colonize individual crypts lined with mucosal epithelial cells. **(d)** One of two Fluid Processing Cassettes (FPC) that housed either the symbiotic or aposymbiotic animals for the duration of the experiment. **(e)** individual Aquarium bags that each housed eight replicate juvenile squid connected to pumps in the FPC that would bring fluids in and out of the bag. Bar = 1 cm. **(f)** Diagram of the experimental flow of the spaceflight samples with 16 replicate Aquarium bags at four time points. At the end of the experiment, the FPCs were opened by a crew member, and Aquarium bags were removed and placed at −80 °C until the return to Earth. A replicate experimental flow using the same flight hardware and timeline was completed on the ground as a control.

Animal Care and Use Committees (IACUC). A table of all abbreviations used in this manuscript and their meanings is listed in Table 1.

2.2 Animal husbandry

A breeding colony of adult field-caught *E. scolopes* was maintained at the Space Life Sciences Laboratory in Merritt Island, FL in a recirculating seawater system with a water temperature of ~23 °C and a 12 h:12 h day/night light cycle. Egg clutches were maintained separately in 2.5-gallon aquariums under the same temperature and lighting conditions for the duration of their development. One day before hatching, eggs were placed in individual bowls with aeration, and upon hatching, squid were removed within 1 h and placed into filtered seawater (FSW).

2.3 Bacteria cultures

Approximately 48 h before launch, cultures of *V. fischeri* strain ES114 were grown overnight in Luria broth saline to stationary phase as previously described (Boettcher and Ruby, 1990). Bacteria were rinsed once by centrifuging at 15,000 x g for 1 min, the supernatant removed, and the pellet resuspended in FSW. The resuspended *V. fischeri* were then diluted 1:1000 in FSW for an approximate concentration of 5×10^5 cells per ml of FSW.

2.4 UMAMI spaceflight experimental design and gravity controls

The experiment entitled Understanding of Microgravity on Animal-Microbe Interactions (UMAMI) was performed within the ADvanced Space Experiment Processor (ADSEP) using two Fluid Processing Cassettes (Figure 1d; Supplementary Figure S1) designed and constructed by Redwire Space (Formerly Techshot, Greenville, IN, USA). Each cassette housed eight experimental loops, consisting of three fluorinated ethylene propylene (FEP) 25-mL cell culture bags (Saint-Gobain, Gaithersburg, MD), which are permeable to O_2 and CO_2 but impermeable to water. For each bag, there were two ports connected by Masterflex™ 1/16″ ID tubing made of platinum-cured silicone and two peristaltic pump motors,

TABLE 1 List of abbreviations and meanings used in the manuscript.

Abbreviation	Meaning
ADSEP	Advanced Space Experiment Processor
APO	Aposymbiotic animals without beneficial microbes
CEA	Ciliated epithelium appendages
DAPK	Death-associated protein kinase
DEGs	Differentially expressed genes
ESI	Electrospray ionization
EVT	Equipment verification testing
FDR	False Discovery Rate
FEP	Fluorinated ethylene propylene
FPC	Fluid processing cassette
FSW	Filtered seawater
GSEA	Gene-set enrichment analysis
IACUC	Institutional animal care and use committee
ISS	International Space Station
LBP	Lipopolysaccharide binding proteins
LC-HRMS	Liquid chromatography high-resolution mass spectrometry
NCBI	National center for Biotechnology Information
OPLS-DA	Orthogonal partial least squares discriminant analysis
ORPs	Oxysterol-binding proteins-related proteins
PCA	Principal component analysis
PGRP	Peptidoglycan receptor proteins
RLU	Relative light units
SGS	Significant gene sets
SECIM	Southeastern Center for Integrated Metabolomics
SpX-22	SpaceX Commercial Resupply Services-22
SYM	Symbiotic animals colonized with *V. fischeri*
TMM	Trimmed mean of M-values
UMAMI	Understanding of microgravity on animal-microbe interactions
VIP	Variable importance in projection

one on each end of the bag. The three bags within each of the loops were: 1) Inoculum, 2) Aquarium, and 3) Fixative (Supplementary Figure S1).

Approximately 32 h before launch, the Inoculum bags were readied by loading either 5 mL of *V. fischeri* inoculum for the symbiotic (SYM) colonization condition or 5 mL FSW for the aposymbiotic (APO) colonization condition. Each of the Aquarium bags was prepared by loading eight squid hatchlings into the FEP bags containing 25 mL of FSW. The Fixative bags contained 25 mL of RNAlater™ (ThermoFisher Scientific, Waltham, MA, USA). There were two sets of FEP bags per treatment enabling 16 biological replicates and two technical replicates. Once the bags were aseptically assembled, they were connected to the appropriate pump and tested to ensure no leakage. All APO loops were contained separately in FPC module A, whereas all SYM loops were contained in FPC module B to ensure no potential in-flight contamination by *V. fischeri*. ADSEP hardware was turned over to SpaceX 24 h prior to launch. The temperature was maintained at 23 °C ± 0.5 for the duration of the UMAMI experiment.

Approximately 7.5 h after the successful launch of SpaceX CRS-22, but before the Dragon capsule docked to the International Space Station (ISS), the UMAMI experiment was successfully run for a duration of 12 h. The UMAMI experiment was automatically controlled by Redwire Space from their headquarters in Greenville, IN. The experimental sequence in the ADSEP FPC cassettes initiated with a backflow of 5 mL of FSW from the Aquarium bags into the Inoculum bags to enable the mixing of the culture and provide space in the Aquarium bags for the inoculum (SYM) or seawater control (APO). Following the backflow, the colonization step was initiated by pumping 5 mL of inoculum into the Aquarium bags resulting in a final colonization of 1×10^5 cells per mL of FSW. In the APO cassette, 5 mL of FSW was added to the Aquarium bags. The colonization step was allowed to incubate for 0, 2, 6, or 12 h. After colonization, approximately 24 mL of FSW was pumped out of the Aquarium bag back into the Inoculation bags, which were then renamed the Waste bags after which 24 mL of RNALater was added to the Aquarium bags to arrest transcription in the host squid and prevent tissue degradation. This approach was used to increase the ratio of RNALater to water ratio and improve tissue fixation. The fixation process took approximately 2 min. Following the conclusion of the UMAMI experimental procedure, the cassettes were cooled to 10 °C for 48 h until the bags could be manually removed by a crewmember and frozen at −80 °C on the ISS. The Aquarium bags containing RNALater were stored on the ISS for 30 days at −80 °C until their return to Earth.

As a control, the entire procedure, including the 39.5-h hold (32 h pre-launch and 7.5 h transit time), was repeated at the Space Life Science Laboratory under unit gravity conditions at 23 °C. Upon completion of the control experiment, the sample bags were removed from the cassette and placed at −80 °C for storage for 30 days. During postflight processing of the spaceflight and gravity controls, the frozen squid were thawed, photographed, placed into fresh RNAlater, and stored at −80 °C until processing.

2.5 Extraction of RNA and sequencing

Light organs were dissected from 16 squid per treatment and pooled in groups of four to provide enough material for RNA extraction. Total RNA was extracted as previously described from each group enabling three RNA extractions per treatment (Koch et al., 2020a). Briefly, RNA was isolated using the RNeasy Kit (Qiagen, Hilden, Germany) and treated with the TURBO DNA-free KitTM (ThermoFisher Scientific, Waltham, MA, USA). The concentration of RNA for each biological replicate was determined using a Qubit 2.0 fluorometer (ThermoFisher Scientific, Waltham, MA, USA). RNA quality was determined with an Agilent 2100 Bioanalyzer using an RNA 6000 Nano Kit (Agilent Technologies, Palo Alto, CA, USA). Normalized RNA samples (5 ng per sample) then underwent library preparation using the

Illumina low input RNA-Seq library prep (Illumina, San Diego, CA) and sequencing using 2 × 150 bp paired-end read sequencing on the Illumina NovaSeq6000 Sequencing system using an S4 flowcell. Both the library preparation and sequencing were performed at the University of Florida ICBR NextGen DNA Sequencing Core Facility (RRID:SCR_019152). After RNASeq analysis, remaining RNA (5 ng) from the replicate 12 h symbiotic flight animals was converted to cDNA and examined with digital PCR (BioRad QX200) using an QiAcuity 26K well plate with EvaGreen Supermix and 16S rRNA gene primers designed to *V. fischeri* (Hoffmann et al., 2010).

2.6 Gene expression analysis

All gene expression analyses were performed using default parameters or as otherwise noted. The resulting sequencing reads first underwent quality verification using FastQC (version 0.11.7) (Andrews, 2014). The reads were then mapped to the *E. scolopes* genome (Belcaid et al., 2019; Schmidbaur et al., 2022) using the splice-aware aligner STAR (version 2.7.9a) (Dobin and Gingeras, 2015) with the minimum mapped length adjusted to 0.5 (i.e., --outFilterMatchNminOverLread and--outFilterScoreMinOverLread set to 0.5).

After mapping, gene expression was quantified using RSEM (version 1.3.3) (Li and Dewey, 2011). The gene expression counts were normalized by Trimmed Mean of M-values (TMM) and samples were compared using an exact test and p-values adjusted for multiple comparisons with the Benjamini–Hochberg method using edgeR (version 3.14.0) (Robinson et al., 2010). Significant differential gene expression was defined as a false discovery rate (FDR) < 0.1. Genes were first characterized using BLASTX (Altschul et al., 1990) against the National Center for Biotechnology Information (NCBI) nonredundant protein sequence database and InterProScan (version 5) against the InterPro 100.0 database (Jones et al., 2014). Characterized genes then underwent gene ontology (GO) mapping and functional annotation using Blast2GO Pro (Gotz et al., 2008) in Omicsbox (version 2.2.4).

For functional analysis of the gene expression, gene-set enrichment analysis (GSEA) was performed (Subramanian et al., 2005) to show GO functions that were significantly over or underrepresented for the condition of interest (e.g., SYM versus APO). The GSEA was performed using a ranked list factoring both fold change and p-value for each gene with the calculation sin (logFC) * -log10 (p-value) and 1000 permutations.

2.7 Extraction and analysis of small molecules

Light organs were dissected from each squid, placed into individual 1.5 mL Eppendorf tubes, frozen at −80 °C, and later analyzed at the University of Florida's Southeast Center for Integrated Metabolomics (SECIM). Frozen samples were thawed on ice, after which one pre-chilled 3 mm stainless steel bead was added to the tube. Next, 50 µL of 5 mM ammonium acetate was added and the samples were vortexed using five cycles that included 10 s vortexing with 5 min incubation on ice. The samples then underwent two additional cycles of vortexing for 10 s and cooling on ice for 3.5 min. The sides of the tubes were washed by adding 50 µL of 5 mM ammonium acetate and then the tubes were centrifuged at 3260 *g* for 2 min at 4 °C. The supernatants (100 µL) were transferred to 5 mL glass conical centrifuge tubes. Next, 5 µL of the Splash Lipidomix internal standard mix (Avanti Polar Lipids, Alabaster, AL), diluted in half, was added. A blank tube was included as an extraction blank.

A biphasic extraction was then conducted following the Folch method where 1200 µL of a 2:1 mixture of ice-cold chloroform: methanol was added to each tube. The tubes were allowed to cool on ice for 20 min with vortexing at 10 min. Next, 100 µL of water was added to each tube and they were allowed to cool again on ice for 10 min with vortexing at 5 min, after which they were centrifuged at 3260 *g* for 10 min at 4 °C. The bottom layer (800 µL) was removed and transferred to a new glass tube with a screw cap. The aqueous portion was re-extracted by adding 400 µL of ice cold 2: 1 chloroform:methanol, vortexed, cooled for 10 min at 4 °C, and again centrifuged at 3260 × 6 for 10 min, 4 °C. At this point, 200 µL of the bottom layer was removed and added to the original organic layer, whereas remaining aqueous portion was saved for later metabolomic processing. The organic layer was dried under a gentle stream of nitrogen at 30 °C. The dried residue was reconstituted in 50 µL of 2-propanol containing the lipid injection standards, vortexed and centrifuged at 3260 × 6 for 10 min, 4 °C. The reconstituted samples were then transferred to an LC vial with fused insert for liquid chromatography high-resolution mass spectrometry (LC-HRMS) analysis.

The aqueous portions were transferred to microcentrifuge tubes and centrifuged at 20,000 x g for 10 min, 4 °C to pellet any remaining protein. Only 250 µL of the supernatant was transferred and 5 µL of the metabolomics internal standard mix was added and vortex mixed (Safari Yazd et al., 2023). The samples were then centrifuged again at 20,000 x g for 10 min, 4 °C. The supernatants were transferred to new microcentrifuge tubes and dried under a gentle stream of nitrogen at 30 °C. The dried residue was then reconstituted with 50 µL of water containing injection standards, vortexed and centrifuged at 20,000 x g for 10 min, 4 °C. The samples were then transferred to plastic LC vials with inserts for analysis.

2.8 Metabolomics and lipidomics using LC-HRMS

All analyses were conducted using LC-HRMS on a Thermo Q Exactive using heated electrospray ionization with both positive and negative ion modes collected using separate injections. The source conditions for lipid analysis were 3.5 kV spray voltage, 5 (+mode) and 15 (-mode) arb units for auxiliary gas, 30 (+mode) and 25 (-mode) arb units for sheath gas, 1 (+mode and 0 (-mode) arb units for sweep gas, 300 °C capillary temperature, and S-lens set to 35. The conditions for metabolomics were 3.5 (+mode) and 3.0 kV (-mode) spray voltage, 10 arb units for auxiliary gas, 50 arb units for sheath gas, 1.0 arb units for sweep gas and S-lens set to 30. Samples were maintained at 9 °C in an autosampler.

Lipids were separated on a Waters Aquity BEH C18 column (1.7 µm, 2.1 mm × 50 mm) with temperature set to 50 °C. Mobile phase A was 60:40 acetonitrile:water with 10 mM ammonium formate and 0.1% formic acid and mobile phase B was 90:8:2 2-propanol:acetonitrile:water also with 10 mM ammonium formate and 0.1% formic acid. The flow rate was 500 µL/min and a multistep

gradient was used. Exact gradient conditions were followed according to previous work (Garrett et al., 2023). Data were collected with a mass resolution setting of 70,000 for full scan mode and a setting of 35,000 for top five data dependent MS/MS (ddMS2). Lipidmatch was used for data compilation and lipid identification (Koelmel et al., 2017). The injection volume was 3 µL for positive ions and 5 µL for negative ions.

Metabolites were separated using an ACE-Excel C18-pfp column (2.0 µm, 2.1 mm × 100 mm, Mac-Mod Chadds Ford, PA) with temperature set to 25 °C and flow rate of 350 µL/min. Mobile phase A was 0.1% formic acid in water and mobile phase B was acetonitrile. The gradient was held at 100% A from 0–3 min, then increased to 80% B from 3–13 min, held constant at 80% B for 3 min, returned to initial conditions in 0.5 min. The flow rate was increased to 600 µL/min from 16.5–20 min to re-equilibrate the column. The flow rate was returned to 350 µL/min at 20 min and then held until 22.5 min before the next injection. The injection volume was 2 µL (positive ions) and 4 µL (negative ions). Data processing was conducted by converting the files to mzXML using MSconvert from ProteoWizard (Chambers et al., 2012) then loaded into MZmine 2.53 where a batch method was used for peak picking, alignment, and metabolite identification using an internal retention time library of 1200 metabolites (5 ppm for positive, 10 ppm for negative, ∓ 0.25 min retention time window) for level 1 identification.

2.9 Statistics and reproducibility

Statistical analysis of principal components analysis PCA was conducted using a T2 hotelling test, which is a multivariate extension of the t-test and evaluated whether the two groups are significantly different in a multivariate space (Conesa et al., 2008). Statistical significance for the GSEA was defined as the default FDR q-value <0.25. Significant gene sets were ordered by the normalized enrichment score (NES), which indicates how much a gene set is overrepresented at the top or the bottom of the ranked list and is normalized for multiple comparisons. PERMANOVA and k-means analyses for all datasets were performed on the normalized data that was log-transformed.

All statistical comparisons of the small molecule analysis were performed using Metaboanalyst 5.0 (Xia et al., 2009). Prior to statistical analysis, the metabolite and lipid datasets were normalized by sum, log-transformed, and underwent Pareto scaling. The normalized data was then visualized PCA and outliers outside of the 95% confidence intervals were removed. Orthogonal partial least squares discriminant analysis (OPLS-DA) was used to initially identify potentially significant molecules (VIP >1.5), which were then confirmed using a Student's t-test adjusted for multiple comparisons (FDR <0.1).

3 Results

3.1 Spaceflight experimental overview and hardware performance validation

The experiment entitled Understanding of Microgravity on Animal-Microbe Interactions (UMAMI) was designed to monitor the initiation and early developmental pathways of the host animal in the presence and absence of beneficial microbes in the spaceflight environment. The UMAMI experiment was completed in two fluid processing cassettes (Figure 1d), one with *V. fischeri* (i.e., symbiotic, SYM) and one without *V. fischeri* (i.e., aposymbiotic, APO) and integrated into the ADSEP where it was launched aboard SpX-22 from the Kennedy Space Center. A detailed overview of the experimental design is provided in the methods section and visualized in Figure 1 and Supplementary Figure S1. Briefly, the automated experiment used a loop design where animals were housed within cell culture bags (i.e., aquariums; Figure 1e) and upon reaching microgravity motors pumped in either filtered-sterilized seawater containing *V. fischeri* inoculant as SYM or only filtered seawater as APO controls. Animals were then incubated as SYM or APO for 0, 2, 6, or 12 h and then were infiltrated with RNALater to terminate the experiment and the bags were later moved to −80 °C aboard the ISS until their return to Earth 30 days later (Figure 1f). This entire procedure was repeated under normal gravity conditions as a ground control. A total of 16 replicate animals were recovered for each colonization treatment with two technical replicates for both the spaceflight experiment (n = 128) and ground controls (n = 128).

Electrical current draws and temperature readings from the ADSEP hardware suggested motor and pumping operations for both the spaceflight and ground controls occurred as planned (Supplementary Figure S2). The temperature for the spaceflight and ground incubations ranged from 22.78 °C to 23.32 °C for the APO cassettes and 22.80 °C–23.67 °C for the SYM cassettes, indicating less than 1 °C fluctuation for the duration of the UMAMI experiment.

To confirm that animals were effectively inoculated using the ADSEP hardware, replicate experiments, including the 39-h hold simulating the launch pad experience, were conducted on the ground during the Experiment Verification Test (Schulze et al., 2020), a NASA requirement to ensure spaceflight readiness. The entire inoculation and incubation protocol was carried out but before the final RNALater fixation step, the experiment was then stopped at 12 h, and the live animals from all timepoints were removed from the fluid processing cassettes and aquarium bags to assess the effectiveness of colonization within the hardware. At all timepoints individual animals in the SYM and APO conditions were assessed for luminescence, colony forming units, and bacteria-induced apoptosis (Supplementary Figure S3). EVT results at 12 h indicated that the SYM animals exhibited significantly higher luminescence readings (2000 - 22,000 relative light units (RLU); $p < 0.0001$) compared to APO controls (<500 RLU) suggesting effective colonization by the bioluminescent symbiont using the automated ADSEP hardware (Supplementary Figure S3a).

Additionally, a subsample of SYM light organs in the EVT exhibiting high luminescence were subsequently homogenized and plated on seawater tryptone media resulting in a minimum of 2×10^5 cells per light organ, thereby confirming colonization by *V. fischeri* (Supplementary Figure S3b). APO light organs exhibited no colony forming units when plated. SYM light organs also exhibited the hallmarks of apoptosis with distinct patterns of pycnotic nuclei within the superficial ciliated epithelium of the light organ compared to APO controls (Supplementary Figure S3c). Together, these results

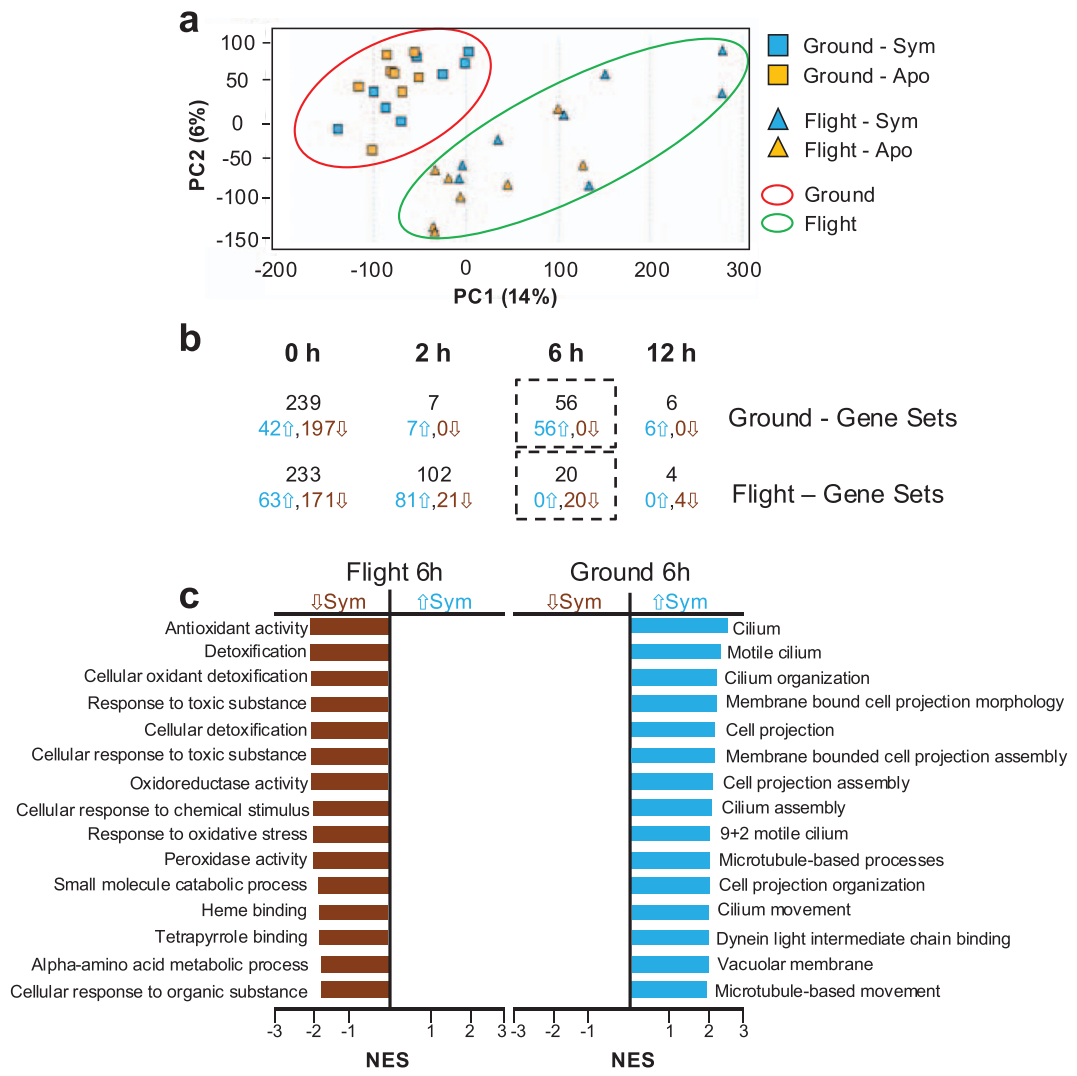

FIGURE 2
Comparison of transcriptome data from the UMAMI flight experiment. **(a)** Principal component (PC) analysis of 32 transcriptomes derived from the aposymbiotic (Apo, orange) and symbiotic (Sym, blue) exposed to either spaceflight (triangle) or ground (square) conditions. The transcriptomes were clustered into two distinct groups including ground samples (red circle) and flight samples (green circle). Ellipses reflect 95% confidence that the data falls within the boundaries. **(b)** Gene set enrichment (GSEA) comparisons of transcriptomes derived from ground controls and flight samples at each time point of the experiment. Total number of significant gene sets are in black. Numbers of enriched gene sets in symbiotic animals relative to aposymbiotic animals are marked in blue, whereas genes that are decreased in symbiotic animals relative to aposymbiotic animals are listed in orange. **(c)** Histogram of GSEA analysis comparisons at 6 h post-inoculation depicting the distinct categories that are either enriched (blue) or decreased (Petrash et al., 2012) according to the normalized enrichment score (NES) in symbiotic animals compared to aposymbiotic animals.

suggest that the UMAMI experimental design, ADSEP hardware, and automated procedures were effective in inoculating the animals with *V. fischeri* during EVT testing.

For spaceflight animals, hardware limitations did not enable luminescence levels or the rates of colonization to be monitored during flight; however, the presence of *V. fischeri* was directly measured post-flight with digital PCR using 16S rRNA gene primers designed for *V. fischeri* (Hoffmann et al., 2010). Remaining RNA derived from 12 h SYM flight light organs were examined with digital PCR indicating that, as in the ground EVT testing, host animals were effectively colonized with *V. fischeri* by 12 h (Supplementary Figure S3d) mirroring previous spaceflight results using the squid-vibrio model system (Casaburi et al., 2017).

3.2 Transcriptome analyses revealed spaceflight was the primary driver of differential gene expression in the host tissues regardless of symbiotic state

To investigate the effects of spaceflight and bacterial colonization on host gene expression, RNA sequencing was used to generate a total of 23,064,220,236 raw reads across 32 samples with a mean of 720,756,882 reads per sample. The reads were then mapped to the *E. scolopes* genome (Belcaid et al., 2019; Schmidbaur et al., 2022) with a success rate of 65%–77% reads per sample. A PERMANOVA test was conducted on the transcriptome to statistically compare experimental groups. Strong statistical significance was found between the spaceflight and ground

datasets (p-value <0.0001), whereas the aposymbiotic and symbiotic datasets displayed little to no significance (p-value = 0.064). Additionally, a k-means analysis was conducted on the entire transcriptome and suggested the data separates according to the spaceflight condition, with a single ground cluster and three spaceflight clusters (Supplementary Figure S4). Analysis of the transcriptomes using principal component analysis (PCA) revealed two distinct clusters, one each for flight and ground samples (Figure 2a). Collectively, these results suggest there is more variability in the spaceflight exposed animals compared to the ground controls and that spaceflight may be imprinting a stress that affects both the magnitude and variability in gene expression within the host animal.

Although the specific rate of light organ colonization was not directly measured due to spaceflight hardware limitations, gene expression markers typically associated with the initiation of symbiosis were examined and compared at all time points and treatments. Transcripts of target genes that encode for peptidoglycan receptor proteins (PGRPs), galaxins, cathepsin-L, and lipopolysaccharide binding proteins (LBPs), which all typically exhibit trends of increased expression during the normal colonization under unit gravity conditions (Krasity et al., 2011; Krasity et al., 2015; Heath-Heckman et al., 2016; Peyer et al., 2018), were examined. Both flight and ground controls exhibited a non-significant, but overall trend of increased gene expression of several genes typically associated with colonization with low, but consistent upregulation in SYM animals relative to APO across most time points (Supplementary Figure S5). The exception was transcripts of genes encoding cathepsin-Ls, which were increased under APO conditions beginning at 2 h only during spaceflight conditions (Supplementary Figure S5). Cathepsins are known to be activated by caspases (Zheng et al., 2008), which can be increased under the stress of simulated microgravity conditions (Vroom et al., 2022), suggesting cathepsins are not a useful marker of symbiosis during spaceflight. However, the increased expression of other genes that are typically associated with the onset of symbiosis in the spaceflight and ground experiments in SYM animals compared to APO controls reinforce that the host tissues were colonized by *V. fischeri* during the spaceflight.

Due to the large effect of spaceflight on overall gene expression in the host tissues gene expression analysis was performed on the flight and ground samples separately. To examine the effect of bacterial colonization on host gene expression under spaceflight and ground conditions, the SYM and APO transcriptomes were compared at each time point with differentially expressed genes (DEGs) defined as those under a false discovery rate (FDR) of 0.1 (Supplementary Figure S6; (Supplementary Dataset S1). At the beginning of the experiment during spaceflight (t = 0 h), the ratio of DEGs up or downregulated under SYM and APO conditions was approximately even (i.e., the same number of DEGs increased in SYM and APO) (Supplementary Figure S6a). However, as the experiment progressed there were fewer significant DEGs increased under SYM conditions relative to APO. This apparent gene downregulation in SYM began at 2 h post-inoculation and continued at 6 h and 12 h. Similar results were observed in ground-based simulated microgravity conditions where APO animals exhibited much higher transcriptional activity than SYM animals (Casaburi et al., 2017). Overall, the increased transcriptional activity during the spaceflight within aposymbiotic animals suggests that in the absence of the microbe the animal is activating a range of unique host gene expression responses to the novel environment of spaceflight that was not observed under ground controls. The presence of the symbiotic microbe in the spaceflight environment might "override" or help mitigate this increase of transcriptional activity within the animals.

3.3 Gene set enrichment analyses revealed that several key animal developmental pathways were altered during spaceflight and dependent on the presence or absence of symbionts

To identify common gene functions beyond just DEGs affected by colonization under spaceflight conditions, gene-set enrichment analysis (GSEA) was performed at all time points with significant gene sets (SGSs) defined with the default value of FDR <0.25 (Figures 2b,c; Supplementary Figure S7; Supplemental Dataset S2 - S3). GSEA uses a ranked list of genes that incorporates both the p-value and fold change in the expression to find gene functions that are statistically over- or underrepresented within the dataset (Mootha et al., 2003; Subramanian et al., 2005). A comparison of the SGSs at the start of the experiment (t = 0 h) revealed that the spaceflight and ground animal transcriptomes shared 30.8% of the SGS despite the flight animals being launched into space (Figure 2b).

By 2 h post inoculation of the animals, however, there were few common SGS between the spaceflight and ground controls (Figure 2b; Supplemental Dataset S3). Under normal gravity conditions, there was an initial drop in overall SGSs at 2 h (Figure 2b), which matches gene expression patterns previously published in studies on the host animal (Chun et al., 2008; Moriano-Gutierrez et al., 2019). By 6 h in ground controls, many of the SGSs that were enriched in SYM animals (Figure 2c; Supplemental Dataset S3) had functions associated with previously characterized bacteria-induced morphogenesis of the ciliated epithelium (Montgomery and McFall-Ngai, 1994; Foster and McFall-Ngai, 1998; Foster et al., 2000). In spaceflight-exposed animals, however, at 2 h there were 102 SGSs enriched compared with only 7 SGSs in ground controls, with 81 SGSs increased in SYM and 21 increased in APO (Figure 2b; Supplementary Figure S7). Furthermore, gene sets associated with bacteria-induced morphogenesis were enriched earlier in spaceflight conditions relative to ground controls (i.e., 2 h in flight and 6 h in ground controls), suggesting the host responded transcriptionally to the bacteria more rapidly in spaceflight than under unit gravity conditions (Figure 2c; Supplementary Figure S7; Supplemental Dataset S3).

3.4 Symbiotic animals exhibited lower oxidative stress gene expression in spaceflight compared to aposymbiotic controls

One pronounced difference in the spaceflight animals was the enrichment of SGSs associated with oxidative stress in the light organs of APO animals, which did not receive their symbiotic microbes. Analysis of the gene expression of core and noncore genes associated with oxidative stress pathways revealed dynamic changes under spaceflight conditions (Figures 3a,d; Supplemental Dataset S2-S3).

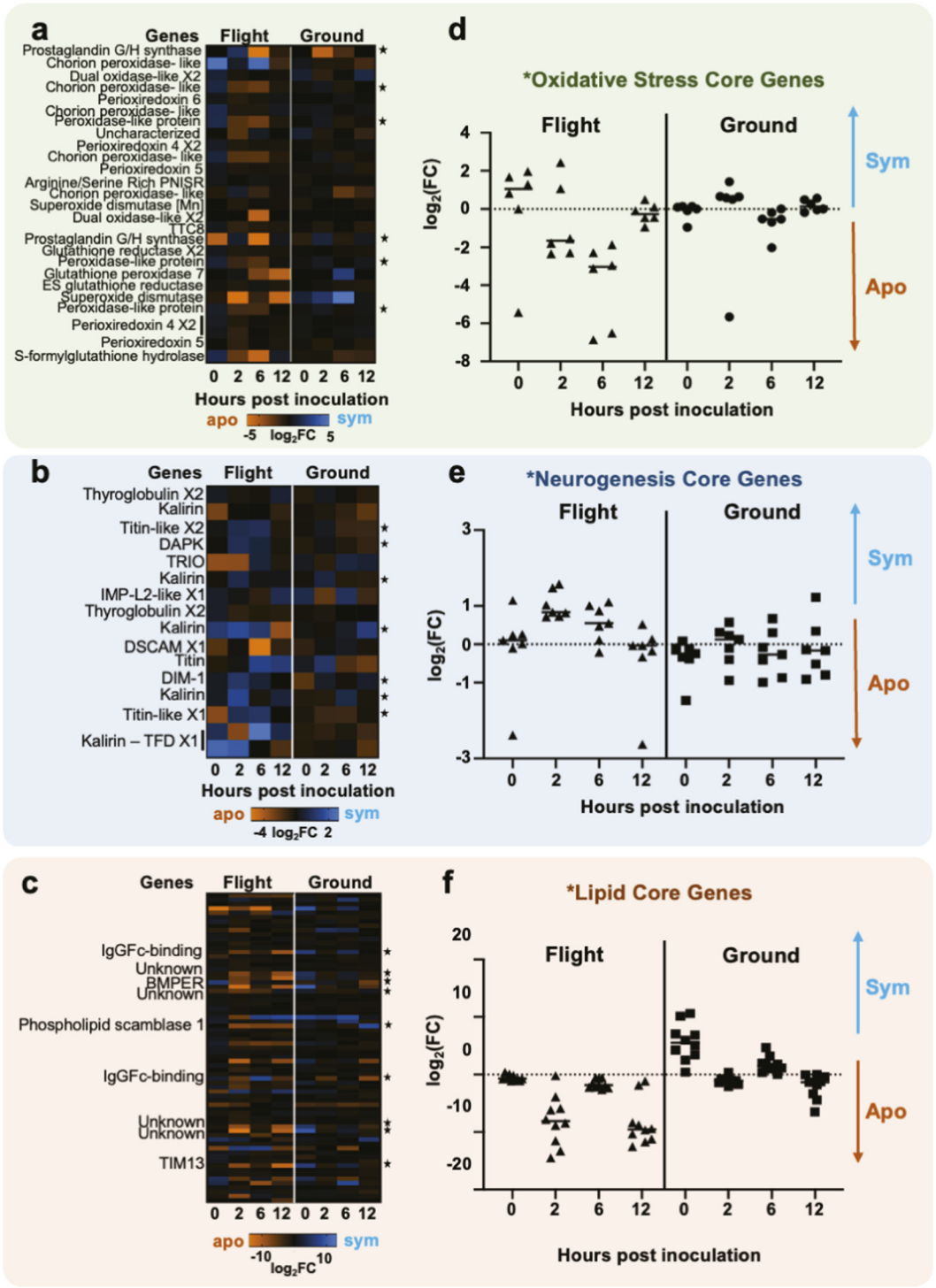

FIGURE 3
Targeted comparison of gene set enrichment analysis for oxidative stress, neurogenesis, and lipid transport genes in host transcriptomes. Heat maps depicting the expression of transcripts for genes associated with **(a)** oxidative stress, **(b)** neurogenesis, and **(c)** lipid transport that were either enriched in symbiotic (sym, blue) or aposymbiotic (apo, orange) animals under both spaceflight (Perez-Riverol et al., 2016) or ground conditions. Numbers represent the hours post-inoculation with either *Vibrio fischeri* (sym) or filtered seawater (apo). Asterisks represent core genes within the oxidative stress gene set. Scatter plots of the fold change in expression of core genes associated with **(d)** oxidative stress, **(e)** neurogenesis, and **(f)** lipid transport over time that either increased under symbiotic (sym) or aposymbiotic (apo) conditions.

At the start of the experiment (t = 0), there was a slight increase in the expression of oxidative stress genes in spaceflight animals relative to their ground controls, but by 2 h post-inoculation, there was a reduction in the levels of gene expression in the SYM animals that persisted for the rest of the experimental timeline. During spaceflight, genes encoding several enzymatic antioxidants, such as

superoxide dismutase and a wide range of peroxidases (e.g., glutathione peroxidases, glutathione reductase, and peroxiredoxins) exhibited increased expression in APO animals relative to SYM animals beginning at 2 h (Figure 3a) and continued through 6 h (Supplemental Dataset S2 – S3). These results suggest that aposymbiotic animals exhibited a higher and sustained oxidative stress transcriptional response in their light organs during spaceflight compared to symbiotic animals.

3.5 Symbiotic animals exhibited higher expression of genes associated with neurogenesis and cell morphogenesis under spaceflight conditions

Numerous gene sets associated with the formation and stabilization of synaptic connections as well as the regulation of microtubule assembly and neuronal differentiation were significantly enriched in the SYM light organs compared to APO during spaceflight (Figure 2c). Several recent studies have shown the important role that symbiotic microbes can have in regulating the blood-brain barrier, homeostatic regulation of neuronal cells and in neurogenesis (Ogbonnaya et al., 2015; Sharon et al., 2016). Beginning at 2 h post-inoculation, there were increases in genes encoding for several kalirin-like and Trio proteins (Figures 3b,e; Supplemental Dataset S2 – S3), which play important roles in nerve growth, remodeling of synapses, and axonal development (Paskus et al., 2020). The increased expression of these genes in SYM animals during spaceflight was also observed at 6 h post-inoculation, however, by 12 h post-inoculation expression levels of most of these genes were at background levels suggesting transient, but increased, gene transcription during spaceflight.

Additionally, there was also a significant increase ($P < 0.05$) in expression of death-associated protein kinase (DAPK) early (i.e., 2 h) in the initiation of the symbiosis during spaceflight that was not significant under ground conditions (Figure 3b). DAPK is a molecular switch that has many different roles within animals including mediating ceramide and caspase-induced apoptosis (Pelled et al., 2002; Jin and Gallagher, 2003). DAPK also has important roles in regulating neuronal death, regulating synaptic plasticity, and is upregulated during recovery from injury (Wang et al., 2017; Farag and Roh, 2019). There was also increased expression of titin isoforms during spaceflight in SYM animals, which encode proteins found in numerous muscles and neuronal cell types (Goffena et al., 2018; Cameron et al., 2024) and has been shown to regulate the structure of microvilli and trafficking of animal immune cells (Toffali et al., 2023). These results suggest that during spaceflight microbes can regulate aspects of neurogenesis during the bacteria-induced morphogenesis of the host light organ tissue.

3.6 Aposymbiotic animals exhibited higher transcription of genes associated with lipid production, transport, and localization during spaceflight

In animals that never received their beneficial symbiont, there were pronounced increases relative to SYM in the expression of genes associated with lipid transport and localization genes during spaceflight. Although many of the genes that were differentially expressed during spaceflight encode hypothetical or uncharacterized proteins, there were increases in the expression of genes associated with lipid transport proteins, such the oxysterol-binding proteins-related proteins (ORPs), apolipophorins, phospholipid scramblases, sterol-regulated proteins, and IgGFc-binding proteins (Figures 3c,f). Many of these lipid-transport proteins, such as apolipophorin and phospholipid scramblases, have dual functions and can bind microbial-associated molecular patterns, such as LPS and phosphatidylserines, as well as serve as mediators of apoptosis, innate immunity, oxidative stress responses, and other signaling processes in host cells (Whitten et al., 2004; Kodigepalli et al., 2015; Slone et al., 2015). Additionally, IgGFc-binding proteins, also known as Fc gamma binding proteins, are mucin-like glycoproteins that play roles in mucosal defense and are often secreted into the mucus to increase the structural integrity of the mucus layer (Ehrencrona et al., 2021; Gorman et al., 2023). The significant increase of transcripts that encode for these diverse lipid transport proteins in the APO animals during spaceflight may reflect a heightened stress response from animals that did not receive the normal microbial signals or cues for development.

3.7 Spaceflight altered the host lipidome with increases in ceramide abundance in symbiotic animals

In parallel with the transcriptomic analysis, the lipidome of the host animals was also profiled for each treatment and time point. Liquid chromatography/high-resolution mass spectrometry (LC/HRSM) with electrospray ionization (ESI) detected 3612 total peaks in positive ESI mode and 1812 total peaks in negative ESI, with 938 (~26%) and 373 (~21%), respectively, able to be characterized (Figure 4; Supplementary Figure S8; Supplemental Dataset S4). Principal component analysis showed that, as with the transcriptome, spaceflight strongly affected the lipidome at all time points. To characterize differential lipid abundances, a combination of multivariate orthogonal partial least squares discriminant analysis (OPLS-DA) and univariate (Student's t-test) statistical tests were used with significant lipids being defined as having both a VIP >1.5 for OPLS-DA and FDR <0.1 for the t-test (Figure 4a; Supplementary Figure S8). In normal gravity conditions, there was an initial enrichment of significant lipids (both positive and negative ESI) in SYM animals relative to APO at 0 h and 2 h, followed by a reversal in the pattern (i.e., APO > SYM) at 6 h and 12 h (Figures 4b,c; Supplementary Figure S8). Beginning at 2 h in spaceflight, the majority of significant lipids exhibited a trend of being increased in SYM which continued at 6 h. Interestingly, significantly different lipids during spaceflight were only found at 12 h in SYM in the -ESI mode (Supplementary Figure S8).

Of those lipids that could be identified with tandem mass spectrometry (MS/MS), ceramides were the most abundant group, representing 36.6% and 41.7% of characterized lipids in flight and ground, respectively (Figure 4c; Supplemental Dataset S4). During spaceflight, ceramides were generally increased in SYM animals relative to APO with the highest levels at 2 and 6 h post-inoculation (Supplementary Figure S9). In ground conditions at 2 h, however, the abundance of ceramides was evenly distributed between APO and SYM animals but by 6 and 12 h ceramides

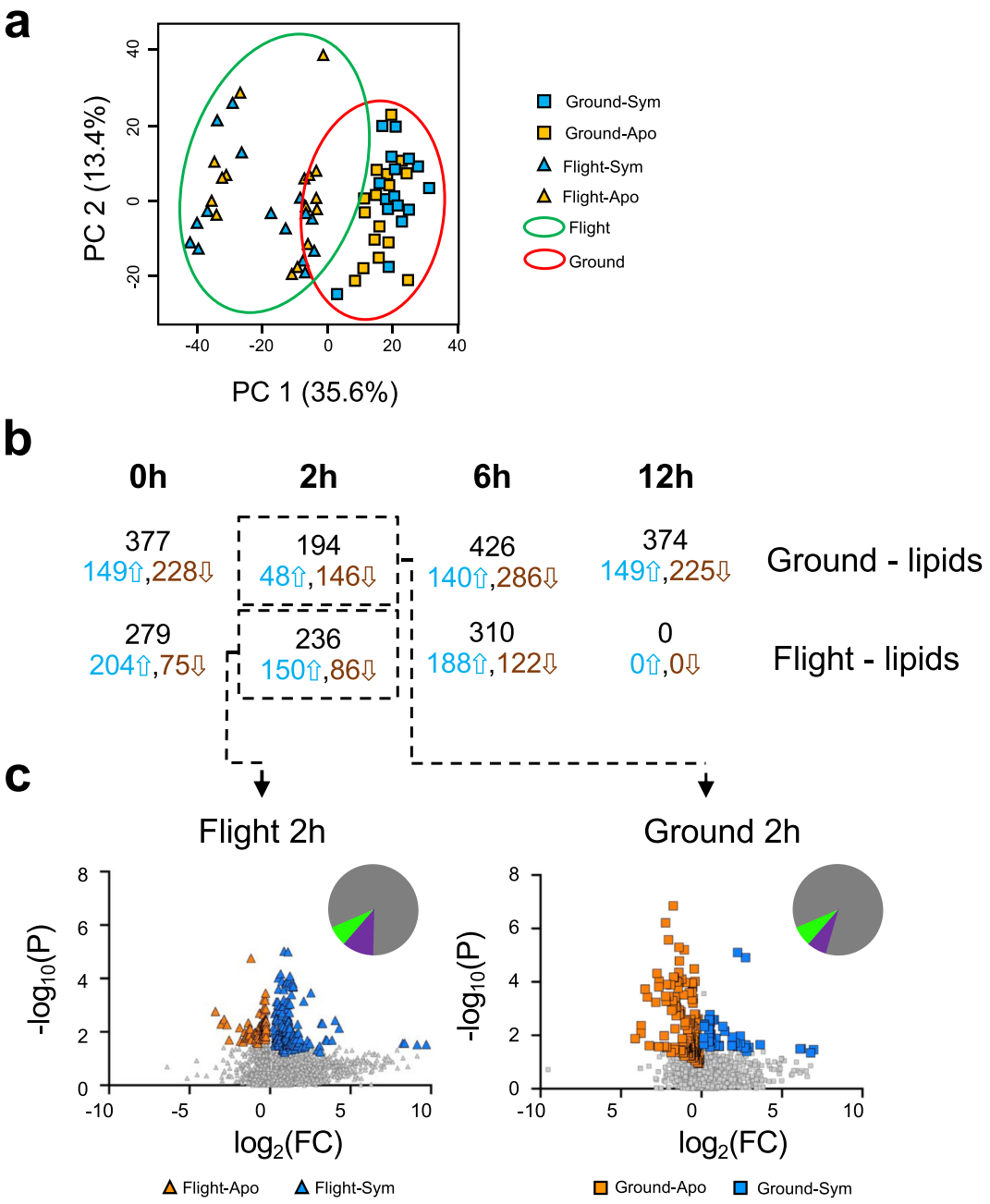

FIGURE 4
Comparison of host lipidome during spaceflight in the presence and absence of symbiotic microbes. **(a)** Principal component (PC) analysis of the positive electrospray ionization mass spectroscopy (ESI-MS) lipidome data depicting the differences between the flight (triangle) and ground (square) conditions of symbiotic (blue) and aposymbiotic (Petrash et al., 2012) animals. Ellipses reflect 95% confidence that the data falls within the boundaries. **(b)** Timeline of differentially abundant lipids under spaceflight and ground conditions. For each time point, the top number reflects the total amount of significant lipids (VIP> 1.5, FDR <0.1), the lower numbers indicate the amount of lipids that are either significantly increased (blue) or decreased (Petrash et al., 2012) in symbiotic (Sym) relative to aposymbiotic (Apo) animals. **(c)** Volcano plots of lipids detected at 2 h comparing Sym and Apo under flight (left) and ground (right) conditions. All recovered lipids from the positive-ESI data were plotted and each symbol represents one unique lipid. The log fold change (Goffena et al., 2018) is represented on the x-axis, whereas the -$\log_{10}$ of the p-value (P) is on the y-axis. Significant lipids (VIP> 1.5, FDR <0.1) are indicated with blue (up in Sym > Apo) or orange (Apo > Sym), whereas non-significant lipids are in gray. The pie charts (inset) indicate the biochemical characterization of the significant lipids separated into three groupings: unknowns (dark gray), ceramides (green), and miscellaneous (purple).

exhibited greater abundance in the APO animals compared to symbiotic animals (Supplementary Figure S9).

Ceramides are lipid modulators that regulate a wide range of functions in the cell, including cell differentiation, cell arrest, inflammation, and apoptosis (Uchida and Park, 2021). Accumulation of ceramides within cells can affect membrane fluidity, alter mitochondrial function, and induce both extrinsic and intrinsic apoptosis pathways (Boojar et al., 2018) primarily

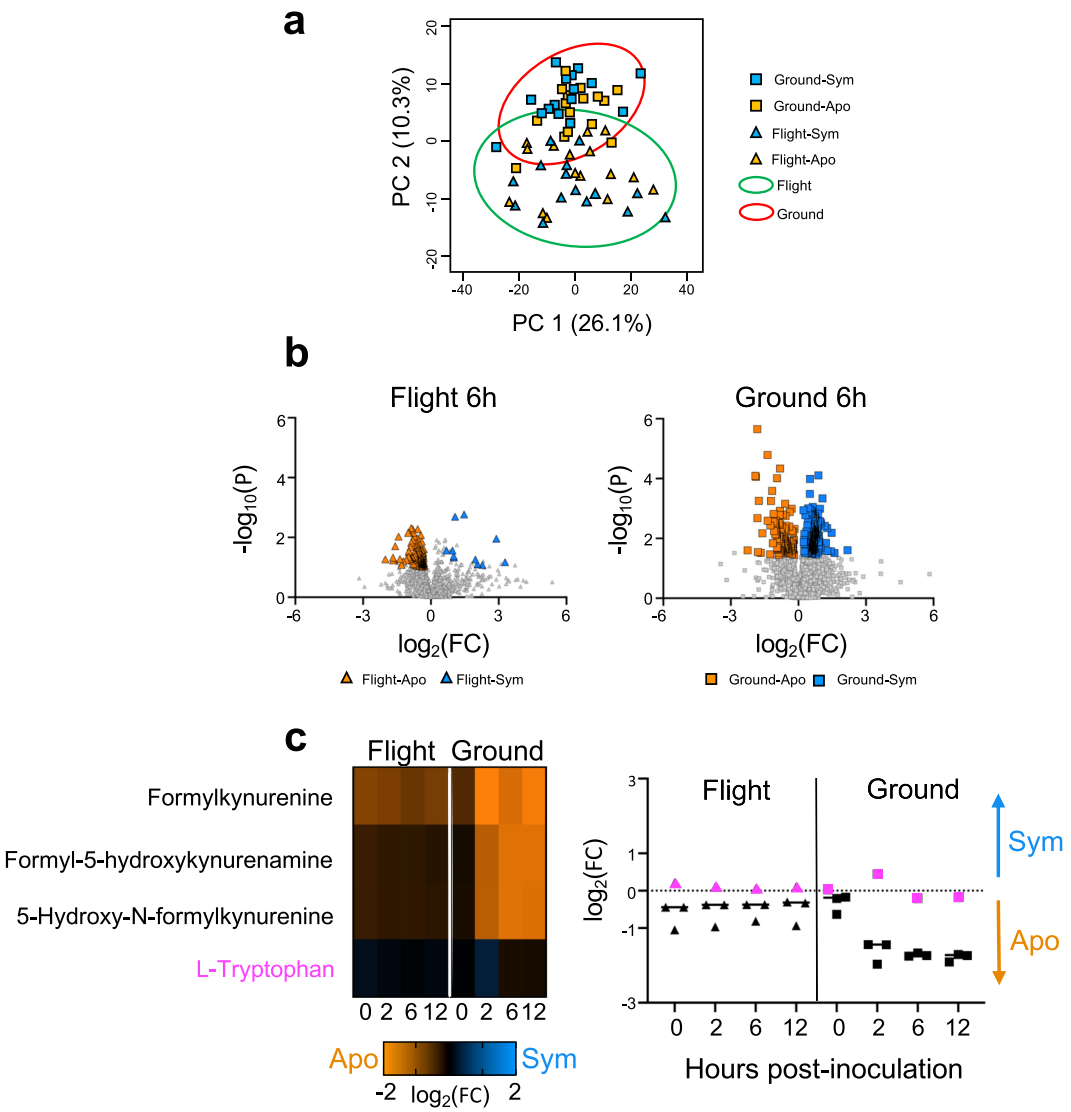

FIGURE 5
Comparison of host metabolome during spaceflight in the presence and absence of symbiotic microbes. **(a)** Principal component (PC) analysis of the positive electrospray ionization mass spectroscopy (ESI-MS) metabolome data depicting the differences between the flight (triangle) and ground (square) conditions of symbiotic (blue) and aposymbiotic (Petrash et al., 2012) animals. Ellipses reflect 95% confidence that the data falls within the boundaries. **(b)** Volcano plots of metabolites detected at 2 h, comparing symbiotic (Sym) and aposymbiotic (Apo) animals under spaceflight (left) and ground (right) conditions. All recovered features from the positive-ESI data were plotted and each symbol represents one metabolite. The $\log_2$-fold change (Goffena et al., 2018) calculated as Sym/Apo is represented on the x-axis, whereas the $-\log_{10}$ of the p-value (P) is on the y-axis. Statistically significant metabolites (VIP >1.5, FDR <0.1) are indicated in blue (Sym > Apo) or orange (Apo > Sym), whereas non-significant metabolites are in gray. **(c)** Heat map (left) of metabolites associated with the kynurenine pathway under flight and ground conditions. The $\log_2$-fold change calculated as Sym/Apo is displayed to show enrichment under symbiotic (blue) or aposymbiotic conditions (Petrash et al., 2012). A scatter plot of the same metabolites over time depicting metabolite enrichment in Sym (blue) relative to Apo (Petrash et al., 2012) animals under flight (triangle) or ground (square) conditions. The $\log_2$-fold change (Goffena et al., 2018) calculated as Sym/Apo is represented on the y-axis and the time of sampling post-inoculation is on the x-axis. Pink symbols reflect L-tryptophan abundance across all time points and conditions.

through the activation of caspases (Pilatova et al., 2023). The elevated levels of ceramides in SYM light organs during spaceflight coupled with the observed decreases of transcription in genes associated with lipid transport (Figure 3c) suggest ceramides, as well as other lipids, may be accumulating in the light organs of symbiotic animals during spaceflight. The accumulation of this potent signaling molecule during spaceflight may be causing, and accelerating, several downstream effects, such as increases in initiator and executioner caspase gene expression and early onset of bacteria-induced apoptosis previously observed in ground-based simulated microgravity experiments (Foster et al., 2013; Vroom et al., 2022).

3.8 Symbiotic state altered metabolites associated with the regulation of the host immune system during spaceflight

To assess how spaceflight impacted the overall pool of metabolites within the host light organ, untargeted metabolomics using LC/HRMS was used to generate profiles of the different

treatments. Analysis revealed a total of 3500 peaks in positive ESI (+ESI) and 818 peaks in negative ESI (-ESI) mode (Supplementary Dataset S5). Of the recovered metabolites, 129 (~4%) for + ESI and 55 (~7%) for -ESI could be annotated at the highest confidence identification (level 1). Principal component analysis showed that as in the transcriptome and lipidome the metabolome was strongly influenced by spaceflight (Figure 5a).

Statistical analysis of metabolites was performed using OPLS-DA and a Student's t-test, with significant metabolites being defined as having both a VIP >1.5 and FDR <0.1, respectively (Supplementary Dataset S4; Supplementary Figures S10-S11). Analysis of the +ESI data revealed that at the start of the UMAMI experiment (t = 0), the metabolome profiles of the animals in spaceflight and ground conditions were comparable (Supplementary Figure S10). By 2 h post-inoculation, however, there was a pronounced disparity in both the +ESI and -ESI data in SYM animals between spaceflight and ground samples with a reduction in the significant metabolites observed in spaceflight samples compared to ground controls (Figure 5b; Supplementary Figures S10 – S11).

Although most of the significant metabolites could not be fully identified to the highest level of confidence, the molecules that could be characterized with high confidence possessed similar bioactivities related to the modulation of the host immune system. For example, by 2 h in spaceflight conditions, metabolites known to act as immunostimulants were increased in APO animals relative to SYM animals, including mevalonolactone and azelaic acid (Supplemental Dataset S5) (Gratton et al., 2018; Proietti et al., 2020; Izbicka and Streeper, 2021). Additionally, in APO animals there were significant increases in formylkynurenine, formyl-5-hydroxykynurenamine, and 5-hydroxy-N-formylkynurenine, which are metabolites involved in the kynurenine pathway (Figure 5c; Supplemental Dataset S5).

The kynurenine pathway is critical for tryptophan catabolism and is highly regulated by the immune system (Adams et al., 2012). Under high oxidative stress and inflammation conditions, the kynurenine pathway can act as a negative feedback system to help scavenge reactive oxygen species and suppress the inflammatory response through tryptophan depletion (Seo and Kwon, 2023). Metabolites associated with the kynurenine pathway were increased in APO in both conditions relative to SYM, however, the differences due to symbiotic state were lower under flight conditions compared to ground controls (Figure 5c; Supplementary Dataset S5). These results were corroborated by increases in the expression of genes associated with tryptophan metabolism (e.g., tryptophanase isoforms, tryptophan 2,3-diooxygenase; and kynurenine 3-monooxygenase) in the APO animals during spaceflight beginning 2 h after the start of the experiment (Supplementary Figure S6). These data may reflect the host attempting to compensate for the lack of symbiotic microbes by increasing expression of host-derived tryptophanases. Interestingly, tryptophan abundance was maintained approximately equal between APO and SYM animals under both spaceflight and ground conditions (Figure 5c; Supplementary Dataset S5). There was, however, a pronounced reduction in the accumulation of kynurenine pathway metabolites in APO animals under spaceflight compared to ground controls (Figure 5c; Supplemental Dataset S5). The reduction of the immunosuppressive kynurenine pathway in the APO flight animals may increase the stress environment in the APO light organs during spaceflight.

In contrast, the SYM animals exhibited elevated levels of immunosuppressant metabolites, such as urocanate and xanthine, which were increased 6 h post-inoculation in SYM animals relative to APO controls (Figure 5b; Supplemental Dataset S5). Additionally, the decrease in kynurenine-pathway metabolites in SYM animals relative to APO suggests that *V. fischeri* played a major role in regulating tryptophan metabolism, perhaps through the metabolization of tryptophan (Wei et al., 2021) along the kynurenine pathway during spaceflight, thereby modulating the oxidative stress and immune responses in the host during spaceflight. Overall, these results may suggest that colonization of the light organ by the symbiont may act as a "calming" mechanism for host stress and the innate immune response during spaceflight.

4 Discussion

Microbes play a major role in maintaining human health and strategies to ensure effective microbiome homeostasis and resilience during long-duration spaceflight are critical. The outcomes of our multi-omics approach, as summarized in Figure 6, suggest that in spaceflight conditions microbes can effectively trigger the activation of key bacteria-induced pathways needed for the natural maturation of host tissues. However, the results also show that the onset of some aspects of normal developmental timeline were altered and accelerated under the stress of spaceflight. Additionally, the results show that the microbes may confer stress resistance to the host to help potentially mitigate perturbations caused by spaceflight. Together, these results suggest there is alteration of the molecular dialog occurring between the host and symbiont, which is an important finding for the field of space biology.

The spaceflight environment has widespread effects on the physiology of animals that can negatively impact host-microbe interactions, including changes in body fluid dynamics, shortening of cilia, reductions in mucin production, and reorganization of the cellular cytoskeleton (Noskov, 2011; Wu et al., 2011; Svalina and Forsman, 2013; Norsk et al., 2015; Ding et al., 2020). Despite these potential challenges, our results suggest that the host was able to effectively recruit *V. fischeri* from the environment and initiate symbiosis under the stress of spaceflight (Supplementary Figure S3d). Much like the mammalian digestive tract where microbes must travel through numerous chemical and physically distinct environments to associate with the surfaces of mucosal epithelial cells (Alvarez-Ordonez et al., 2011), *V. fischeri* physically interface with mucociliary epithelial surfaces of the squid light organ (Figure 1) where they aggregate within a mucus matrix containing antimicrobial molecules that serves to enrich *V. fischeri* from surrounding environmental microbes (Yip et al., 2006; Troll et al., 2010; Altura et al., 2013; Kremer et al., 2013).

Analysis of the host gene expression responses suggests that *V. fischeri* was able induce the key host molecular and biochemical responses in the squid within the UMAMI experimental timeline, suggesting that normal bacteria-induced development of host epithelial tissues will not be impeded during space travel. Additional experimentation, however, will be required to more fully assess whether certain aspects of the colonization processes, such as mucin production, surface-attachment strategies, aggregate formation, and bacterial strain population dynamics are altered

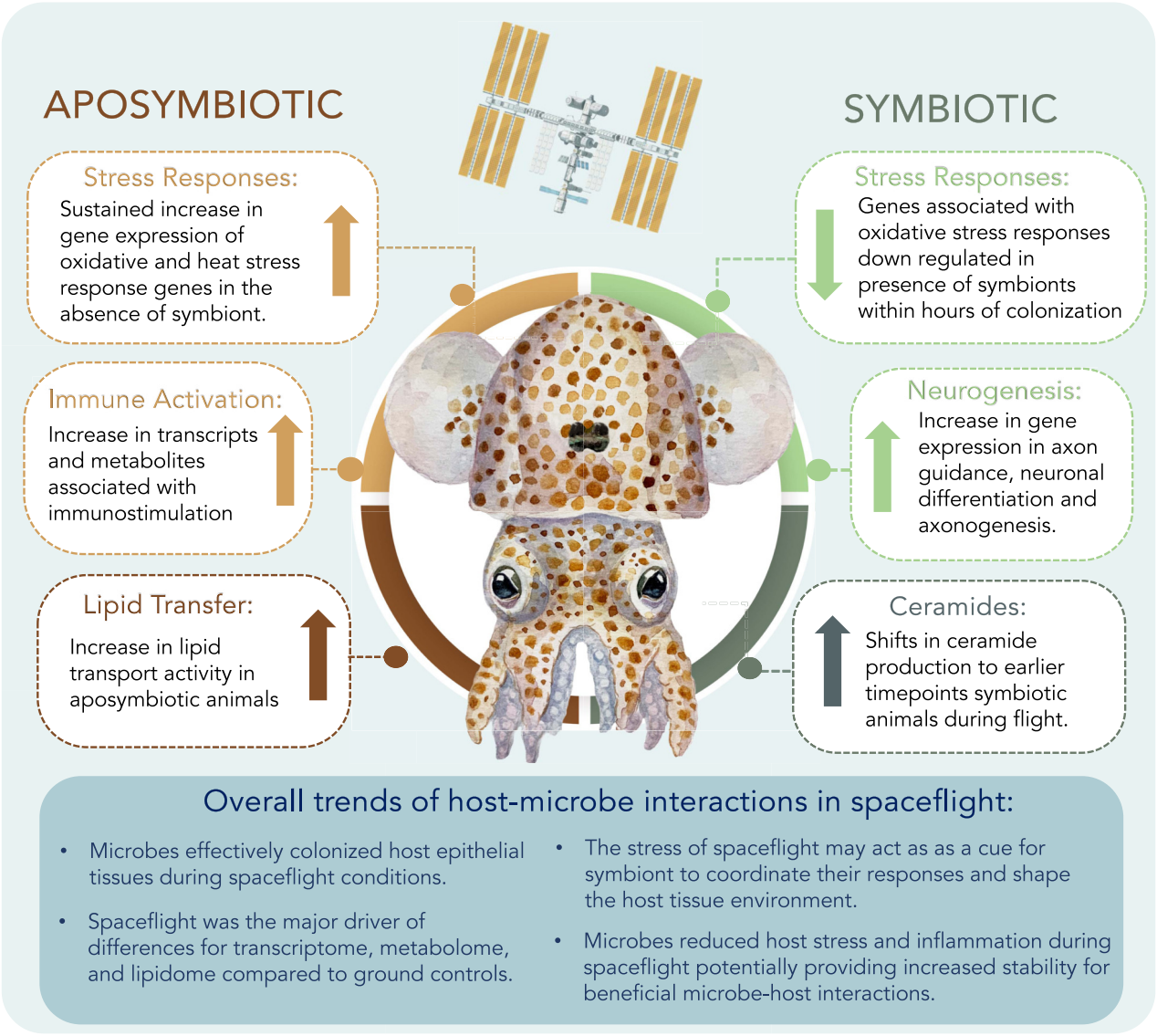

FIGURE 6
Summary figure of the overarching trends within the host light organ in the presence and absence of symbiotic microbes during spaceflight. Overall trends suggest increases and persistence of stress responses of host animals in the absence of symbiosis-competent microbes suggesting microbes may confer resistance to stress during spaceflight. Additionally, symbiotic animals exhibited increases in genes associated with neuronal differentiation and axonogenesis at earlier time points than ground controls suggesting the presence of the bacteria during spaceflight might transcriptionally activate developmental pathways faster than under normal gravity conditions.

during spaceflight, as simulated microgravity has been shown to impact these colonization phenotypes in animal-microbe symbioses *in vivo* (Foster et al., 2013; Vroom et al., 2021; Bongrand and Foster, 2023). For example, it is possible that the rate of bacterial colonization within the host light organ during spaceflight was altered, potentially accounting for many of the observed changes in the host transcriptome, metabolome and lipidome. Future research will also be needed to more carefully assess whether the observed changes in host responses were caused by changes in bacterial physiology *in vivo*. Numerous studies have demonstrated spaceflight can impact the physiology of bacterial cultures (Taylor, 2015; Zea et al., 2017) and can drive changes in microbiome composition and function during spaceflight (Jiang et al., 2019; Urbaniak et al., 2020). Therefore, more research is needed to more fully understand the mechanisms by which spaceflight alters host-microbe communication and colonization dynamics.

In addition to the initiation of colonization, the UMAMI experiment showed that there were several changes to the host developmental timeline during spaceflight, including the rapid onset of an oxidative stress gene expression response. Although no organism on Earth has specifically evolved to cope with spaceflight, the innate immune system of eukaryotes has evolved to sense and respond rapidly to environmental perturbations, such as increases in oxidative stress and colonization by microbes (Schwartzman and Ruby, 2016). There is a long history of spaceflight studies demonstrating that the elevated radiation and

microgravity environment can induce oxidative stress responses throughout all organ systems in the body (Pavlakou et al., 2018). As redox homeostasis is fundamental to all metabolic processes, life has evolved rapid system-wide oxidative stress responses (Sies et al., 2017). The increase in oxidative stress responses in both the symbiotic and aposymbiotic animals after the onset of the UMAMI experiment likely reflects the immediate stress animals experienced in the spaceflight environment. However, within 2 h of colonization by *V. fischeri,* the presence of the microbes appeared to attenuate the magnitude of the stress response to the perturbation of spaceflight. The attenuation of stress responses in symbiotic animals may be a by-product of the bacteria using the host stress response as a cue for normal colonization, thereby stabilizing the symbiosis during spaceflight.

The use of stress to cue and shape host-microbe interactions has a long evolutionary history and is conserved in both plants and animals (Schwartzman and Ruby, 2016). In plants, one well-studied example is in leguminous plants, such as the clover *Medicago truncatula*, whose symbiotic interactions with the nitrogen-fixing *Sinorhizobium meliloti* results in the formation of nodules in the host plant to improve the nutritional environment (Lopez et al., 2008). The host plant can initiate a generalized oxidative stress response that can trigger transcriptional changes in the symbiont to increase extracellular polymeric substances, which coupled with the production of Nod factors, contributes to the formation of an infection thread and the onset of bacteria-induce nodule formation within the plants (Levine et al., 1994; Hirsch et al., 2001). The results of the UMAMI experiment suggest that the spaceflight environment may increase physical and chemical stimuli in the host, such as reactive oxygen species and antimicrobial peptides, acting as cues for the microbial response. Bacteria can then regulate the transcriptional responses of the host subsequently reducing stress and accelerating normal bacteria-induced development.

The impact of the bacterial symbiont on host physiology during spaceflight was also reflected in the lipidome and metabolome analyses. The pronounced increase in lipids in symbiotic animals, in particular ceramides, during spaceflight suggests that bacteria-induced lipid accumulation may be triggering important signaling functions in the host. For example, ceramides can induce a range of physiological responses including, neuronal differentiation, the acceleration of apoptosis signaling, and increased exosome production to mediate communication between different cell types (Fiorani et al., 2023; Zhang et al., 2023; Ding et al., 2024) that are highly dependent on the intracellular location (Kagan et al., 2022). Additionally, changes in the metabolome also revealed the critical role that the bacteria were playing in mediating the host stress response during spaceflight. The changes in metabolites associated with tryptophan metabolism may play a critical role in maintaining, or restoring, the homeostasis of the host light organ during spaceflight. In mammals, regulation of tryptophan metabolite abundance is coordinated between the gut microbiome and intestinal epithelial cells, and the kynurenine pathway and its metabolic derivatives are being targeted as potential therapeutic agents for inflammatory and autoimmune diseases (Seo and Kwon, 2023).

Together, analyses of the transcriptional and small molecule changes in the host tissues revealed the pronounced impact that spaceflight can have on symbiotic interactions. Evidence suggested there was extensive crosstalk between *V. fischeri* and the host tissues during spaceflight at the initiation of the colonization process, and that the bacteria appeared to help the host squid mitigate the stress responses that the aposymbiotic animals exhibited during spaceflight. These results serve as an important foundation for building future strategies to maintain host-symbiont health in closed ecosystems, such as spacecraft. Predicting microbiome homeostasis and resiliency to the perturbations of spaceflight will require an improved understanding of the mechanisms regarding the initiation, establishment, maintenance, and loss of symbiotic interactions with their eukaryotic hosts. Additionally, to support sustainable long-term habitation beyond Earth, more complex holobiomic analyses of how collections of multicellular hosts and their associated microbiomes interconnect will be required to more fully understand the direct and indirect effects of spaceflight on beneficial interactions with microbes.

Data availability statement

The RNA-Seq datasets can be found in Bioproject PRJNA1066592 and accession numbers SRX23333868 - SRX23333899. All other datasets are available in the Supplemental Materials.

Ethics statement

The animal study was approved by the University of Florida (201910899), NASA Flight (SQD01), and the Kennedy Space Center (FLT-20-129) Institutional Animal Care and Use Committees (IACUC). The study was conducted in accordance with the local legislation and institutional requirements.

Author contributions

EK: Investigation, Validation, Writing – review and editing, Methodology, Data curation, Writing – original draft, Formal Analysis, Visualization. AC: Investigation, Writing – original draft, Methodology, Writing – review and editing, Formal Analysis. TG: Methodology, Data curation, Investigation, Writing – review and editing, Writing – original draft, Validation, Formal Analysis. RO: Investigation, Writing – review and editing, Writing – original draft, Supervision, Methodology, Validation. RB: Investigation, Writing – review and editing, Methodology, Writing – original draft. DR: Investigation, Writing – review and editing, Writing – original draft, Conceptualization, Methodology. JF: Visualization, Resources, Formal Analysis, Funding acquisition, Writing – original draft, Project administration, Investigation, Supervision, Methodology, Writing – review and editing, Conceptualization.

Funding

The author(s) declared that financial support was received for this work and/or its publication. This work was supported by a NASA Space Biology Award 80NSSC19K0138 awarded to J.S.F.

Acknowledgements

The authors thank Dr. Megan MacArthur for her technical assistance aboard the International Space Station.

Conflict of interest

Authors RO, RB, and DR were employed by Redwire Space Technologies, Inc.

The remaining author(s) declared that this work was conducted in the absence of any commercial or financial relationships that could be construed as a potential conflict of interest.

Generative AI statement

The author(s) declared that generative AI was not used in the creation of this manuscript.

Any alternative text (alt text) provided alongside figures in this article has been generated by Frontiers with the support of artificial intelligence and reasonable efforts have been made to ensure accuracy, including review by the authors wherever possible. If you identify any issues, please contact us.

Publisher's note

Supplementary material

The Supplementary Material for this article can be found online at: https://www.frontiersin.org/articles/10.3389/frspt.2026.1791484/full#supplementary-material

References

Adams, S., Braidy, N., Bessede, A., Brew, B. J., Grant, R., Teo, C., et al. (2012). The kynurenine pathway in brain tumor pathogenesis. *Cancer Res.* 72, 5649–5657. doi:10.1158/0008-5472.CAN-12-0549

Afshinnekoo, E., Scott, R. T., MacKay, M. J., Pariset, E., Cekanaviciute, E., Barker, R., et al. (2020). Fundamental biological features of spaceflight: advancing the field to enable deep-space exploration. *Cell* 183, 1162–1184. doi:10.1016/j.cell.2020.10.050

Altschul, S. F., Gish, W., Miller, W., Myers, E. W., and Lipman, D. J. (1990). Basic local alignment search tool. *J. Mol. Biol.* 215, 403–410. doi:10.1016/S0022-2836(05)80360-2

Altura, M. A., Heath-Heckman, E. A., Gillette, A., Kremer, N., Krachler, A. M., Brennan, C., et al. (2013). The first engagement of partners in the *euprymna scolopes-Vibrio fischeri* symbiosis is a two-step process initiated by a few environmental symbiont cells. *Environ. Microbiol.* 15, 2937–2950. doi:10.1111/1462-2920.12179

Alvarez-Ordonez, A., Begley, M., Prieto, M., Messens, W., Lopez, M., Bernardo, A., et al. (2011). *Salmonella* spp. survival strategies within the host gastrointestinal tract. *Microbiol. Read.* 157, 3268–3281. doi:10.1099/mic.0.050351-0

Andrews, S. (2014). FastQC a quality-control tool for high-throughput sequence data *Ac*. uk/projects/fastqc.

Avila-Herrera, A., Thissen, J., Urbaniak, C., Be, N. A., Smith, D. J., Karouia, F., et al. (2020). Crewmember microbiome May influence microbial composition of ISS habitable surfaces. *PLoS One* 15, e0231838. doi:10.1371/journal.pone.0231838

Bedree, J. K., Kerns, K., Chen, T., Lima, B. P., Liu, G., Ha, P., et al. (2023). Specific host metabolite and gut microbiome alterations are associated with bone loss during spaceflight. *Cell Rep.* 42, 112299. doi:10.1016/j.celrep.2023.112299

Belcaid, M., Casaburi, G., McAnulty, S. J., Schmidbaur, H., Suria, A. M., Moriano-Gutierrez, S., et al. (2019). Symbiotic organs shaped by distinct modes of genome evolution in cephalopods. *Proc. Natl. Acad. Sci. U. S. A.* 116, 3030–3035. doi:10.1073/pnas.1817322116

Blaber, E., Marcal, H., and Burns, B. P. (2010). Bioastronautics: the influence of microgravity on astronaut health. *Astrobiology* 10, 463–473. doi:10.1089/ast.2009.0415

Boettcher, K. J., and Ruby, E. G. (1990). Depressed light emission by symbiotic *Vibrio fischeri* of the sepiolid squid *euprymna scolopes*. *J. Bacteriol.* 172, 3701–3706. doi:10.1128/jb.172.7.3701-3706.1990

Bongrand, C., and Foster, J. S. (2023). Modeled microgravity impacts *Vibrio fischeri* population structure in a mutualistic association with an animal host. *Environ. Microbiol.* 25 (12), 3269–3279. doi:10.1111/1462-2920.16522

Bongrand, C., and Ruby, E. G. (2019). The impact of *Vibrio fischeri* strain variation on host colonization. *Curr. Opin. Microbiol.* 50, 15–19. doi:10.1016/j.mib.2019.09.002

Bongrand, C., Koch, E. J., Moriano-Gutierrez, S., Cordero, O. X., McFall-Ngai, M., Polz, M. F., et al. (2016). A genomic comparison of 13 symbiotic *Vibrio fischeri* isolates from the perspective of their host source and colonization behavior. *ISME J.* 10, 2907–2917. doi:10.1038/ismej.2016.69

Boojar, M. M. A., Boojar, M. M. A., Golmohammad, S., and Bahrehbar, I. (2018). Data on cell survival, apoptosis, ceramide metabolism and oxidative stress in A-494 renal cell carcinoma cell line treated with hesperetin and hesperetin-7-O-acetate. *Data Brief.* 20, 596–601. doi:10.1016/j.dib.2018.08.065

Cameron, B., Torres-Hernandez, L., Montague, V. L., Lewis, K. A., Smith, H., Fox, J., et al. (2024). Titin is a nucleolar protein in neurons. *Res. Sq.* 3. doi:10.21203/rs.3.rs-4000799/v1

Casaburi, G., Goncharenko-Foster, I., Duscher, A. A., and Foster, J. S. (2017). Transcriptomic changes in an animal-bacterial symbiosis under modeled microgravity conditions. *Sci. Rep.* 7, 46318. doi:10.1038/srep46318

Chambers, M. C., Maclean, B., Burke, R., Amodei, D., Ruderman, D. L., Neumann, S., et al. (2012). A cross-platform toolkit for mass spectrometry and proteomics. *Nat. Biotechnol.* 30, 918–920. doi:10.1038/nbt.2377

Chen, Z., Stanbouly, S., Nishiyama, N. C., Chen, X., Delp, M. D., Qiu, H., et al. (2021). Spaceflight decelerates the epigenetic clock orchestrated with a global alteration in DNA methylome and transcriptome in the mouse retina. *Precis. Clin. Med.* 4, 93–108. doi:10.1093/pcmedi/pbab012

Chun, C. K., Troll, J. V., Koroleva, I., Brown, B., Manzella, L., Snir, E., et al. (2008). Effects of colonization, luminescence, and autoinducer on host transcription during development of the squid-vibrio association. *Proc. Natl. Acad. Sci. U. S. A.* 105, 11323–11328. doi:10.1073/pnas.0802369105

Conesa, A., Bro, R., Garcia-Garcia, F., Prats, J. M., Gotz, S., Kjeldahl, K., et al. (2008). Direct functional assessment of the composite phenotype through multivariate projection strategies. *Genomics* 92, 373–383. doi:10.1016/j.ygeno.2008.05.015

Ding, D., Yang, X., Luan, H. Q., Wu, X. T., Sun, L. W., and Fan, Y. B. (2020). The microgravity induces the ciliary shortening and an increased ratio of anterograde/retrograde intraflagellar transport of osteocytes. *Biochem. Biophys. Res. Commun.* 530, 167–172. doi:10.1016/j.bbrc.2020.06.119

Ding, S., Li, G., Fu, T., Zhang, T., Lu, X., Li, N., et al. (2024). Ceramides and mitochondrial homeostasis. *Cell Signal* 117, 111099. doi:10.1016/j.cellsig.2024.111099

Dobin, A., and Gingeras, T. R. (2015). Mapping RNA-seq reads with STAR. *Curr. Protoc. Bioinformatics* 51, 11.14.11-19

Doino, J. A., and McFall-Ngai, M. (1995). Transient exposures to competent bacteria initiates symbiosis-specific squid light organ morphogenesis. *Biol. Bull.* 189, 347–355. doi:10.2307/1542152

Durante, M., and Cucinotta, F. A. (2008). Heavy ion carcinogenesis and human space exploration. *Nat. Rev. Cancer* 8, 465–472. doi:10.1038/nrc2391

Duscher, A. A., Vroom, M. M., and Foster, J. S. (2024). Impact of modeled microgravity stress on innate immunity in a beneficial animal-microbe symbiosis. *Sci. Rep.* 14, 2912. doi:10.1038/s41598-024-53477-3

Ehrencrona, E., van der Post, S., Gallego, P., Recktenwald, C. V., Rodriguez-Pineiro, A. M., Garcia-Bonete, M. J., et al. (2021). The IgGFc-binding protein FCGBP is secreted

with all GDPH sequences cleaved but maintained by interfragment disulfide bonds. *J. Biol. Chem.* 297, 100871. doi:10.1016/j.jbc.2021.100871

Essock-Burns, T., Bongrand, C., Goldman, W. E., Ruby, E. G., and McFall-Ngai, M. J. (2020). Interactions of symbiotic partners drive the development of a complex biogeography in the squid-vibrio symbiosis. *mBio* 11 (3), 10–1128. doi:10.1128/mBio.00853-20

Essock-Burns, T., Lawhorn, S., Wu, L., McClosky, S., Moriano-Gutierrez, S., Ruby, E. G., et al. (2023). Maturation state of colonization sites promotes symbiotic resiliency in the *euprymna scolopes-Vibrio fischeri* partnership. *Microbiome* 11, 68. doi:10.1186/s40168-023-01509-x

Farag, A. K., and Roh, E. J. (2019). Death-associated protein kinase (DAPK) family modulators: current and future therapeutic outcomes. *Med. Res. Rev.* 39, 349–385. doi:10.1002/med.21518

Fiorani, F., Domenis, R., Dalla, E., Cataldi, S., Conte, C., Mandarano, M., et al. (2023). Ceramide releases exosomes with a specific miRNA signature for cell differentiation. *Sci. Rep.* 13, 10993. doi:10.1038/s41598-023-38011-1

Foster, J. S., and McFall-Ngai, M. J. (1998). Induction of apoptosis by cooperative bacteria in the morphogenesis of host epithelial tissues. *Dev. Genes Evol.* 208, 295–303. doi:10.1007/s004270050185

Foster, J. S., Apicella, M. A., and McFall-Ngai, M. J. (2000). *Vibrio fischeri* lipopolysaccharide induces developmental apoptosis, but not complete morphogenesis, of the *euprymna scolopes* symbiotic light organ. *Dev. Biol.* 226, 242–254. doi:10.1006/dbio.2000.9868

Foster, J. S., Khodadad, C. L., Ahrendt, S. R., and Parrish, M. L. (2013). Impact of simulated microgravity on the normal developmental time line of an animal-bacterial symbiosis. *Sci. Rep.* 3, 1340. doi:10.1038/srep01340

Foster, J. S., Wheeler, R. M., and Pamphile, R. (2014). Host-microbe interactions in microgravity: assessment and implications. *Life* 4, 250–266. doi:10.3390/life4020250

Garrett, T. J., Coatsworth, H., Mahmud, I., Hamerly, T., Stephenson, C. J., Ayers, J. B., et al. (2023). Niclosamide as a chemical probe for analyzing SARS-CoV-2 modulation of host cell lipid metabolism. *Front. Microbiol.* 14, 1251065. doi:10.3389/fmicb.2023.1251065

Garrett-Bakelman, F. E., Darshi, M., Green, S. J., Gur, R. C., Lin, L., Macias, B. R., et al. (2019). The NASA twins study: a multidimensional analysis of a year-long human spaceflight. *Science* 364 (6436), eaau8650. doi:10.1126/science.aau8650

Goffena, J., Lefcort, F., Zhang, Y., Lehrmann, E., Chaverra, M., Felig, J., et al. (2018). Elongator and codon bias regulate protein levels in Mammalian peripheral neurons. *Nat. Commun.* 9, 889. doi:10.1038/s41467-018-03221-z

Gorman, H., Moreau, F., Dufour, A., and Chadee, K. (2023). IgGFc-binding protein and MUC2 mucin produced by colonic goblet-like cells spatially interact non-covalently and regulate wound healing. *Front. Immunol.* 14, 1211336. doi:10.3389/fimmu.2023.1211336

Gotz, S., Garcia-Gomez, J. M., Terol, J., Williams, T. D., Nagaraj, S. H., Nueda, M. J., et al. (2008). High-throughput functional annotation and data mining with the Blast2GO suite. *Nucleic Acids Res.* 36, 3420–3435. doi:10.1093/nar/gkn176

Gratton, R., Tricarico, P. M., Celsi, F., and Crovella, S. (2018). Prolonged treatment with mevalonolactone induces oxidative stress response with reactive oxygen species production, mitochondrial depolarization and inflammation in human glioblastoma U-87 MG cells. *Neurochem. Int.* 120, 233–237. doi:10.1016/j.neuint.2018.05.003

Heath-Heckman, E. A., Foster, J., Apicella, M. A., Goldman, W. E., and McFall-Ngai, M. (2016). Environmental cues and symbiont microbe-associated molecular patterns function in concert to drive the daily remodelling of the crypt-cell brush border of the Euprymna scolopes light organ. *Cell. Microbiol.* 18 (11), 1642–1652. doi:10.1111/cmi.12602

Hirsch, A. M., Lum, M. R., and Downie, J. A. (2001). What makes the rhizobia-legume symbiosis so special? *Plant Physiol.* 127, 1484–1492. doi:10.1104/pp.010866

Hoffmann, M., Brown, E. W., Feng, P. C., Keys, C. E., Fischer, M., and Monday, S. R. (2010). PCR-based method for targeting 16S-23S rRNA intergenic spacer regions among vibrio species. *BMC Microbiol.* 10, 90. doi:10.1186/1471-2180-10-90

Ingber, D. E. (2022). Human organs-on-chips for disease modelling, drug development and personalized medicine. *Nat. Rev. Genet.* 23, 467–491. doi:10.1038/s41576-022-00466-9

Izbicka, E., and Streeper, R. T. (2021). Azelaic acid esters as pluripotent immunomodulatory molecules: nutritional supplements or drugs. *Nutraceuticals* 1, 42–53. doi:10.3390/nutraceuticals1010006

Jiang, P., Green, S. J., Chlipala, G. E., Turek, F. W., and Vitaterna, M. H. (2019). Reproducible changes in the gut microbiome suggest a shift in microbial and host metabolism during spaceflight. *Microbiome* 7, 113. doi:10.1186/s40168-019-0724-4

Jin, Y., and Gallagher, P. J. (2003). Antisense depletion of death-associated protein kinase promotes apoptosis. *J. Biol. Chem.* 278, 51587–51593. doi:10.1074/jbc.M309165200

Jones, P., Binns, D., Chang, H. Y., Fraser, M., Li, W., McAnulla, C., et al. (2014). InterProScan 5: genome-scale protein function classification. *Bioinformatics* 30, 1236–1240. doi:10.1093/bioinformatics/btu031

Kagan, T., Stoyanova, G., Lockshin, R. A., and Zakeri, Z. (2022). Ceramide from sphingomyelin hydrolysis induces neuronal differentiation, whereas *de novo* ceramide synthesis and sphingomyelin hydrolysis initiate apoptosis after NGF withdrawal in PC12 Cells. *Cell Commun. Signal.* 20, 15. doi:10.1186/s12964-021-00767-2

Koch, E. J., and McFall-Ngai, M. (2018). Model systems for the study of how symbiotic associations between animals and extracellular bacterial partners are established and maintained. *Drug Discov. Today Dis. Models* 28, 3–12. doi:10.1016/j.ddmod.2019.08.005

Koch, E. J., Miyashiro, T., McFall-Ngai, M. J., and Ruby, E. G. (2014). Features governing symbiont persistence in the squid-vibrio association. *Mol. Ecol.* 23, 1624–1634. doi:10.1111/mec.12474

Koch, E. J., Bongrand, C., Bennett, B. D., Lawhorn, S., Moriano-Gutierrez, S., Pende, M., et al. (2020a). The cytokine MIF controls daily rhythms of symbiont nutrition in an animal-bacterial association. *Proc. Natl. Acad. Sci. U. S. A.* 117, 27578–27586. doi:10.1073/pnas.2016864117

Koch, E. J., Moriano-Gutierrez, S., Ruby, E. G., McFall-Ngai, M., and Liebeke, M. (2020b). The impact of persistent colonization by *Vibrio fischeri* on the metabolome of the host squid *euprymna scolopes*. *J. Exp. Biol.* 223 (16), jeb212860. doi:10.1242/jeb.212860

Kodigepalli, K. M., Bowers, K., Sharp, A., and Nanjundan, M. (2015). Roles and regulation of phospholipid scramblases. *FEBS Letters* 589, 3–14. doi:10.1016/j.febslet.2014.11.036

Koelmel, J. P., Kroeger, N. M., Ulmer, C. Z., Bowden, J. A., Patterson, R. E., Cochran, J. A., et al. (2017). LipidMatch: an automated workflow for rule-based lipid identification using untargeted high-resolution tandem mass spectrometry data. *BMC Bioinform* 18, 331. doi:10.1186/s12859-017-1744-3

Krasity, B. C., Troll, J. V., Weiss, J. P., and McFall-Ngai, M. J. (2011). Biochemical society transactions LBP/BPI proteins and their relatives: conservation over evolution and roles in mutualism. *Biochem. Soc. Trans.* 39, 1039–1044. doi:10.1042/BST0391039

Krasity, B. C., Troll, J. V., Lehnert, E. M., Hackett, K. T., Dillard, J. P., Apicella, M. A., et al. (2015). Structural and functional features of a developmentally regulated lipopolysaccharide-binding protein. *mBio* 6, e01193–011115. doi:10.1128/mBio.01193-15

Kremer, N., Philipp, E. E., Carpentier, M. C., Brennan, C. A., Kraemer, L., Altura, M. A., et al. (2013). Initial symbiont contact orchestrates host-organ-wide transcriptional changes that prime tissue colonization. *Cell Host Microbe* 14, 183–194. doi:10.1016/j.chom.2013.07.006

Lee, M. D., O'Rourke, A., Lorenzi, H., Bebout, B. M., Dupont, C. L., and Everroad, R. C. (2021). Reference-guided metagenomics reveals genome-level evidence of potential microbial transmission from the ISS environment to an astronaut's microbiome. *iScience* 24, 102114. doi:10.1016/j.isci.2021.102114

Levine, A., Tenhaken, R., Dixon, R., and Lamb, C. (1994). H2O2 from the oxidative burst orchestrates the plant hypersensitive disease resistance response. *Cell* 79, 583–593. doi:10.1016/0092-8674(94)90544-4

Li, B., and Dewey, C. N. (2011). RSEM: accurate transcript quantification from RNA-seq data with or without a reference genome. *BMC Bioinform* 12, 323. doi:10.1186/1471-2105-12-323

Liu, Z., Luo, G., Du, R., Sun, W., Li, J., Lan, H., et al. (2020). Effects of spaceflight on the composition and function of the human gut microbiota. *Gut Microbes* 11, 807–819. doi:10.1080/19490976.2019.1710091

Lopez, M., Herrera-Cervera, J. A., Iribarne, C., Tejera, N. A., and Lluch, C. (2008). Growth and nitrogen fixation in *lotus japonicus* and *Medicago truncatula* under NaCl stress: nodule carbon metabolism. *J. Plant Physiol.* 165, 641–650. doi:10.1016/j.jplph.2007.05.009

Low, L. A., and Giulianotti, M. A. (2019). Tissue chips in space: modeling human diseases in microgravity. *Pharm. Res.* 37, 8. doi:10.1007/s11095-019-2742-0

McFall-Ngai, M., and Bosch, T. C. G. (2021). Animal development in the microbial world: the power of experimental model systems. *Curr. Top. Dev. Biol.* 141, 371–397. doi:10.1016/bs.ctdb.2020.10.002

McFall-Ngai, M. J., and Ruby, E. G. (1991). Symbiont recognition and subsequent morphogenesis as early events in an animal-bacterial mutualism. *Science* 254, 1491–1494. doi:10.1126/science.1962208

McFall-Ngai, M., and Ruby, E. (2021). Getting the message out: the many modes of host-symbiont communication during early-stage establishment of the squid-vibrio partnership. *mSystems* 6, e0086721. doi:10.1128/mSystems.00867-21

Montgomery, M. K., and McFall-Ngai, M. (1993). Embryonic development of the light organ of the sepiolid squid *euprymna scolopes* berry. *Biol. Bull.* 184, 296–308. doi:10.2307/1542448

Montgomery, M. K., and McFall-Ngai, M. (1994). Bacterial symbionts induce host organ morphogenesis during early postembryonic development of the squid *euprymna Scolopes*. *Development* 120, 1719–1729. doi:10.1242/dev.120.7.1719

Mootha, V. K., Lindgren, C. M., Eriksson, K. F., Subramanian, A., Sihag, S., Lehar, J., et al. (2003). PGC-1alpha-responsive genes involved in oxidative phosphorylation are coordinately downregulated in human diabetes. *Nat. Genet.* 34, 267–273. doi:10.1038/ng1180

Mora, M., Wink, L., Kogler, I., Mahnert, A., Rettberg, P., Schwendner, P., et al. (2019). Space station conditions are selective but do not alter microbial characteristics relevant to human health. *Nat. Commun.* 10, 3990. doi:10.1038/s41467-019-11682-z

Moriano-Gutierrez, S., Koch, E. J., Bussan, H., Romano, K., Belcaid, M., Rey, F. E., et al. (2019). Critical symbiont signals drive both local and systemic changes in diel and developmental host gene expression. *Proc. Natl. Acad. Sci. U. S. A.* 116, 7990–7999. doi:10.1073/pnas.1819897116

Moriano-Gutierrez, S., Bongrand, C., Essock-Burns, T., Wu, L., McFall-Ngai, M. J., and Ruby, E. G. (2020). The noncoding small RNA SsrA is released by *Vibrio fischeri* and modulates critical host responses. *PLoS Biol.* 18, e3000934. doi:10.1371/journal.pbio.3000934

Morrison, M. D., Thissen, J. B., Karouia, F., Mehta, S., Urbaniak, C., Venkateswaran, K., et al. (2021). Investigation of spaceflight induced changes to astronaut microbiomes. *Front. Microbiol.* 12, 659179. doi:10.3389/fmicb.2021.659179

Nawroth, J. C., Guo, H., Koch, E., Heath-Heckman, E. A. C., Hermanson, J. C., Ruby, E. G., et al. (2017). Motile cilia create fluid-mechanical microhabitats for the active recruitment of the host microbiome. *Proc. Natl. Acad. Sci. U. S. A.* 114, 9510–9516. doi:10.1073/pnas.1706926114

Norsk, P., Asmar, A., Damgaard, M., and Christensen, N. J. (2015). Fluid shifts, vasodilatation and ambulatory blood pressure reduction during long duration spaceflight. *J. Physiol.* 593, 573–584. doi:10.1113/jphysiol.2014.284869

Noskov, V. B. (2011). Redistribution of body liquids in the conditions of microgravity and simulation of its effects. *Aviakosm. Ekol. Med.* 45, 17–26.

Nyholm, S. V., and McFall-Ngai, M. J. (2004). The winnowing: establishing the squid-vibrio symbiosis. *Nat. Rev. Microbiol.* 2, 632–642. doi:10.1038/nrmicro957

Nyholm, S. V., and McFall-Ngai, M. J. (2021). A lasting symbiosis: how the Hawaiian bobtail squid finds and keeps its bioluminescent bacterial partner. *Nat. Rev. Microbiol.* 19, 666–679. doi:10.1038/s41579-021-00567-y

Nyholm, S. V., Stabb, E. V., Ruby, E. G., and McFall-Ngai, M. J. (2000). Establishment of an animal-bacterial association: recruiting symbiotic vibrios from the environment. *Proc. Natl. Acad. Sci. U. S. A.* 97, 10231–10235. doi:10.1073/pnas.97.18.10231

Nyholm, S. V., Deplancke, B., Gaskins, H. R., Apicella, M. A., and McFall-Ngai, M. J. (2002). Roles of *Vibrio fischeri* and nonsymbiotic bacteria in the dynamics of mucus secretion during symbiont colonization of the *euprymna scolopes* light organ. *Appl. Environ. Microbiol.* 68, 5113–5122. doi:10.1128/aem.68.10.5113-5122.2002

Ogbonnaya, E. S., Clarke, G., Shanahan, F., Dinan, T. G., Cryan, J. F., and O'Leary, O. F. (2015). Adult hippocampal neurogenesis is regulated by the microbiome. *Biol. Psychiatry* 78, e7–e9. doi:10.1016/j.biopsych.2014.12.023

Parafati, M., Giza, S., Shenoy, T. S., Mojica-Santiago, J. A., Hopf, M., Malany, L. K., et al. (2023). Human skeletal muscle tissue chip autonomous payload reveals changes in fiber type and metabolic gene expression due to spaceflight. *NPJ Microgravity* 9, 77. doi:10.1038/s41526-023-00322-y

Paskus, J. D., Herring, B. E., and Roche, K. W. (2020). Kalirin and trio: rhoGEFs in synaptic transmission, plasticity, and complex brain disorders. *Trends Neurosci.* 43, 505–518. doi:10.1016/j.tins.2020.05.002

Pavlakou, P., Dounousi, E., Roumeliotis, S., Eleftheriadis, T., and Liakopoulos, V. (2018). Oxidative stress and the kidney in the space environment. *Int. J. Mol. Sci.* 19 (10), 3176. doi:10.3390/ijms19103176

Pelled, D., Raveh, T., Riebeling, C., Fridkin, M., Berissi, H., Futerman, A. H., et al. (2002). Death-associated protein (DAP) kinase plays a central role in ceramide-induced apoptosis in cultured hippocampal neurons. *J. Biol. Chem.* 277, 1957–1961. doi:10.1074/jbc.M104677200

Perez-Riverol, Y., Gatto, L., Wang, R., Sachsenberg, T., Uszkoreit, J., Leprevost, F. d.V., et al. (2016). Ten simple rules for taking advantage of git and GitHub. *PLoS Comput. Biol.* 12, e1004947. doi:10.1371/journal.pcbi.1004947

Petrash, D. A., Gingras, M. K., Lalonde, S. V., Orange, F., Pecoits, E., and Konhauser, K. O. (2012). Dynamic controls on accretion and lithification of modern gypsum-dominated thrombolites, los roques, Venezuela. *Sediment. Geol.* 245, 29–47. doi:10.1016/j.sedgeo.2011.12.006

Peyer, S. M., Kremer, N., and McFall-Ngai, M. J. (2018). Involvement of a host cathepsin L in symbiont-induced cell death. *MicrobiologyOpen* 7, e00632. doi:10.1002/mbo3.632

Pilatova, M. B., Solarova, Z., Mezencev, R., and Solar, P. (2023). Ceramides and their roles in programmed cell death. *Adv. Med. Sci.* 68, 417–425. doi:10.1016/j.advms.2023.10.004

Proietti, E., Rossini, S., Grohmann, U., and Mondanelli, G. (2020). Polyamines and kynurenines at the intersection of immune modulation. *Trends Immunol.* 41, 1037–1050. doi:10.1016/j.it.2020.09.007

Puschhof, J., Pleguezuelos-Manzano, C., and Clevers, H. (2021). Organoids and organs-on-chips: insights into human gut-microbe interactions. *Cell Host Microbe* 29, 867–878. doi:10.1016/j.chom.2021.04.002

Robinson, M. D., McCarthy, D. J., and Smyth, G. K. (2010). edgeR: a bioconductor package for differential expression analysis of digital gene expression data. *Bioinformatics* 26, 139–140. doi:10.1093/bioinformatics/btp616

Ruby, E. G. (2008). Symbiotic conversations are revealed under genetic interrogation. *Nat. Rev. Microbiol.* 6, 752–762. doi:10.1038/nrmicro1958

Safari Yazd, H., Bazargani, S. F., Fitzpatrick, G., Yost, R. A., Kresak, J., and Garrett, T. J. (2023). Metabolomic and lipidomic characterization of meningioma grades using LC-HRMS and machine learning. *J. Am. Soc. Mass Spectrom.* 34, 2187–2198. doi:10.1021/jasms.3c00158

Schmidbaur, H., Kawaguchi, A., Clarence, T., Fu, X., Hoang, O. P., Zimmermann, B., et al. (2022). Emergence of novel cephalopod gene regulation and expression through large-scale genome reorganization. *Nat. Commun.* 13, 2172. doi:10.1038/s41467-022-29694-7

Schulze, S., Adams, Z., Cerletti, M., De Castro, R., Ferreira-Cerca, S., Fufezan, C., et al. (2020). The archaeal proteome project advances knowledge about archaeal cell biology through comprehensive proteomics. *Nat. Commun.* 11, 1–14. doi:10.1038/s41467-020-16784-7

Schwartzman, J. A., and Ruby, E. G. (2016). Stress as a normal cue in the symbiotic environment. *Trends Microbiol.* 24, 414–424. doi:10.1016/j.tim.2016.02.012

Seo, S. K., and Kwon, B. (2023). Immune regulation through tryptophan metabolism. *Exp. Mol. Med.* 55, 1371–1379. doi:10.1038/s12276-023-01028-7

Septer, A. N., and Stabb, E. V. (2012). Coordination of the arc regulatory system and pheromone-mediated positive feedback in controlling the *Vibrio fischeri* lux operon. *PLoS One* 7, e49590. doi:10.1371/journal.pone.0049590

Sharon, G., Sampson, T. R., Geschwind, D. H., and Mazmanian, S. K. (2016). The central nervous system and the gut microbiome. *Cell* 167, 915–932. doi:10.1016/j.cell.2016.10.027

Sies, H., Berndt, C., and Jones, D. P. (2017). Oxidative stress. *Annu. Rev. Biochem.* 86, 715–748. doi:10.1146/annurev-biochem-061516-045037

Slone, E. A., Pope, M. R., and Fleming, S. D. (2015). Phospholipid scramblase 1 is required for beta2-glycoprotein I binding in hypoxia and reoxygenation-induced endothelial inflammation. *J. Leukoc. Biol.* 98, 791–804. doi:10.1189/jlb.3A1014-480R

Subramanian, A., Tamayo, P., Mootha, V. K., Mukherjee, S., Ebert, B. L., Gillette, M. A., et al. (2005). Gene set enrichment analysis: a knowledge-based approach for interpreting genome-wide expression profiles. *Proc. Natl. Acad. Sci. U. S. A.* 102, 15545–15550. doi:10.1073/pnas.0506580102

Svalina, G., and Forsman, A. D. (2013). The effect of the space flight environment on mucin production in the mouse uterine tube. *Adv. Space Res.* 51, 2229–2234. doi:10.1016/j.asr.2013.01.025

Taylor, P. W. (2015). Impact of space flight on bacterial virulence and antibiotic susceptibility. *Infect. Drug Resist.* 8, 249–262. doi:10.2147/IDR.S67275

Tesei, D., Jewczynko, A., Lynch, A. M., and Urbaniak, C. (2022). Understanding the complexities and changes of the astronaut microbiome for successful long-duration space missions. *Life (Basel)* 12, 495. doi:10.3390/life12040495

Tierney, B. T., Kim, J., Overbey, E. G., Ryon, K. A., Foox, J., Sierra, M. A., et al. (2024). Longitudinal multi-omics analysis of host microbiome architecture and immune responses during short-term spaceflight. *Nat. Microbiol.* 9, 1661–1675. doi:10.1038/s41564-024-01635-8

Toffali, L., D'Ulivo, B., Giagulli, C., Montresor, A., Zenaro, E., Delledonne, M., et al. (2023). An isoform of the giant protein titin is a master regulator of human T lymphocyte trafficking. *Cell Rep.* 42, 112516. doi:10.1016/j.celrep.2023.112516

Troll, J. V., Bent, E. H., Pacquette, N., Wier, A. M., Goldman, W. E., Silverman, N., et al. (2010). Taming the symbiont for coexistence: a host PGRP neutralizes a bacterial symbiont toxin. *Environ. Microbiol.* 12, 2190–2203. doi:10.1111/j.1462-2920.2009.02121.x

Uchida, Y., and Park, K. (2021). Ceramides in skin health and disease: an update. *Am. J. Clin. Dermatol.* 22, 853–866. doi:10.1007/s40257-021-00619-2

Urbaniak, C., Lorenzi, H., Thissen, J., Jaing, C., Crucian, B., Sams, C., et al. (2020). The influence of spaceflight on the astronaut salivary microbiome and the search for a microbiome biomarker for viral reactivation. *Microbiome* 8, 56. doi:10.1186/s40168-020-00830-z

Urbaniak, C., Morrison, M. D., Thissen, J. B., Karouia, F., Smith, D. J., Mehta, S., et al. (2022). Microbial Tracking-2, a metagenomics analysis of bacteria and fungi onboard the international space station. *Microbiome* 10, 100. doi:10.1186/s40168-022-01293-0

Voorhies, A. A., Mark Ott, C., Mehta, S., Pierson, D. L., Crucian, B. E., Feiveson, A., et al. (2019). Study of the impact of long-duration space missions at the international space station on the astronaut microbiome. *Sci. Rep.* 9, 9911. doi:10.1038/s41598-019-46303-8

Vroom, M. M., Rodriguez-Ocasio, Y., Lynch, J. B., Ruby, E. G., and Foster, J. S. (2021). Modeled microgravity alters lipopolysaccharide and outer membrane vesicle production of the beneficial symbiont *Vibrio fischeri*. *Microgravity* 7, 8, doi:10.1038/s41526-021-00138-8

Vroom, M. M., Troncoso-Garcia, A., Duscher, A. A., and Foster, J. S. (2022). Modeled microgravity alters apoptotic gene expression and caspase activity in the squid-vibrio symbiosis. *BMC Microbiol.* 22, 202. doi:10.1186/s12866-022-02614-x

Wang, S., Shi, X., Li, H., Pang, P., Pei, L., Shen, H., et al. (2017). DAPK1 signaling pathways in stroke: from mechanisms to therapies. *Mol. Neurobiol.* 54, 4716–4722. doi:10.1007/s12035-016-0008-y

Wei, G. Z., Martin, K. A., Xing, P. Y., Agrawal, R., Whiley, L., Wood, T. K., et al. (2021). Tryptophan-metabolizing gut microbes regulate adult neurogenesis *via* the aryl hydrocarbon receptor. *Proc. Natl. Acad. Sci. U. S. A.* 118, e2021091118. doi:10.1073/pnas.2021091118

Whitten, M. M., Tew, I. F., Lee, B. L., and Ratcliffe, N. A. (2004). A novel role for an insect apolipoprotein (Apolipophorin III) in beta-1,3-glucan pattern recognition and cellular encapsulation reactions. *J. Immunol.* 172, 2177–2185. doi:10.4049/jimmunol.172.4.2177

Wollenberg, M. S., and Ruby, E. G. (2009). Population structure of *Vibrio fischeri* within the light organs of *euprymna scolopes* squid from two oahu (Hawaii) populations. *Appl. Environ. Microbiol.* 75, 193–202. doi:10.1128/AEM.01792-08

Wu, P. R., Tsai, P. I., Chen, G. C., Chou, H. J., Huang, Y. P., Chen, Y. H., et al. (2011). DAPK activates MARK1/2 to regulate microtubule assembly, neuronal differentiation, and tau toxicity. *Cell Death Differ.* 18, 1507–1520. doi:10.1038/cdd.2011.2

Xia, J., Psychogios, N., Young, N., and Wishart, D. S. (2009). MetaboAnalyst: a web server for metabolomic data analysis and interpretation. *Nucleic Acids Res.* 37, W652–W660. doi:10.1093/nar/gkp356

Yip, E. S., Geszvain, K., DeLoney-Marino, C. R., and Visick, K. L. (2006). The symbiosis regulator RscS controls the *syp* gene locus, biofilm formation and symbiotic aggregation by *Vibrio fischeri*. *Mol. Microbiol.* 62, 1586–1600. doi:10.1111/j.1365-2958.2006.05475.x

Zea, L., Larsen, M., Estante, F., Qvortrup, K., Moeller, R., Dias de Oliveira, S., et al. (2017). Phenotypic changes exhibited by *E. coli* cultured in space. *Front. Microbiol.* 8, 1598. doi:10.3389/fmicb.2017.01598

Zhang, K. R., Jankowski, C. S. R., Marshall, R., Nair, R., Mas Gomez, N., Alnemri, A., et al. (2023). Oxidative stress induces lysosomal membrane permeabilization and ceramide accumulation in retinal pigment epithelial cells. *Dis. Model. Mech.* 16, dmm050066. doi:10.1242/dmm.050066

Zheng, X., Chu, F., Mirkin, B. L., Sudha, T., Mousa, S. A., and Rebbaa, A. (2008). Role of the proteolytic hierarchy between cathepsin L, cathepsin D and caspase-3 in regulation of cellular susceptibility to apoptosis and autophagy. *Biochim. Biophys. Acta* 1783, 2294–2300. doi:10.1016/j.bbamcr.2008.07.027